Development of High-Specificity Fluorescent Probes to Enable Cannabinoid Type 2 Receptor Studies in Living Cells

Roman C. Sarott,[a] Matthias V. Westphal,[a] Patrick Pfaff,[a] Claudia Korn,[b] David A. Sykes,[c] Thais Gazzi,[d] Benjamin Brennecke,[d] Kenneth Atz,[b] Marie Weise,[d] Yelena Mostinski,[d] Pattarin Hompluem,[c] Eline Koers,[c] Tamara Miljuš,[c] Nicolas J. Roth,[e] Hermon Asmelash,[e] Man C. Vong,[c] Jacopo Piovesan,[c] Wolfgang Guba,[b] Arne C. Rufer,[b] Eric A. Kusznir,[b] Sylwia Huber,[b] Catarina Raposo,[b] Elisabeth A. Zirwes,[b] Anja Osterwald,[b] Anto Pavlovic,[b] Svenja Moes,[b] Jennifer Beck,[b] Irene Benito-Cuesta,[f] Teresa Grande,[f] Samuel Ruiz de Martín Esteban,[f] Alexei Yeliseev,[g] Faye Drawnel,[b] Gabriella Widmer,[b] Daniela Holzer,[b] Tom van der Wel,[h] Harpreet Mandhair,[i] Cheng-Yin Yuan,[j] William R. Drobyski,[k] Yurii Saroz,[l] Natasha Grimsey,[l] Michael Honer,[b] Jürgen Fingerle,[b] Klaus Gawrisch,[g] Julian Romero,[f] Cecilia J. Hillard,[m] Zoltan V. Varga,[g,n] Mario van der Stelt,[h] Pal Pacher,[g] Jürg Gertsch,[i] Peter J. McCormick,[e] Christoph Ullmer,[b] Sergio Oddi,[o,p] Mauro Maccarrone,[p,q] Dmitry B. Veprintsev,[c] Marc Nazaré,[d] Uwe Grether,*[b] and Erick M. Carreira*[a]

[a]Laboratorium für Organische Chemie, Eidgenössische Technische Hochschule Zürich, Vladimir-Prelog-Weg 3, 8093 Zürich, Switzerland

[b]Roche Pharma Research & Early Development, Roche Innovation Center Basel, F. Hoffmann-La Roche Ltd., 4070 Basel, Switzerland

[c]Faculty of Medicine & Health Sciences, University of Nottingham, Nottingham NG7 2UH, UK; Centre of Membrane Proteins and Receptors (COMPARE), University of Birmingham and University of Nottingham, Midlands, UK

[d]Leibniz-Institut für Molekulare Pharmakologie FMP, Campus Berlin-Buch, 13125 Berlin, Germany

[e]William Harvey Research Institute, Barts and the London School of Medicine, Queen Mary University of London, London EC1M 6BQ, England

[f]Faculty of Experimental Sciences, Universidad Francisco de Vitoria, Pozuelo de Alarcón, 28223, Madrid, Spain

[g]National Institute on Alcohol Abuse and Alcoholism, National Institutes of Health, Rockville, MD 20852, USA

[h]Department of Molecular Physiology, Leiden Institute of Chemistry, Leiden University, 2333 CC, Leiden, The Netherlands

[i]Institute of Biochemistry and Molecular Medicine, University of Bern, 3012 Bern, Switzerland

[j]Department of Microbiology and Immunology, Neuroscience Research Center, Medical College of Wisconsin, Milwaukee, WI 53226, USA

[k]Department of Medicine, Neuroscience Research Center, Medical College of Wisconsin, Milwaukee, WI 53226, USA

[l]Department of Pharmacology and Clinical Pharmacology, School of Medical Sciences, Faculty of Medical and Health Sciences, University of Auckland, 1142 Auckland, New Zealand

[m]Department of Pharmacology and Clinical Pharmacology, Neuroscience Research Center, Medical College of Wisconsin, Milwaukee, WI 53226, USA

[n]HCEMM-SU Cardiometabolic Immunology Research Group, Department of Pharmacology and Pharmacotherapy, Semmelweis University, 1085 Budapest, Hungary

[o]Faculty of Veterinary Medicine, University of Teramo, 64100 Teramo, Italy

[p]European Center for Brain Research (CERC)/Santa Lucia Foundation, 00179 Rome, Italy

[q]Department of Applied Clinical and Biotechnological Sciences, University of L'Aquila, 67100 L'Aquila, Italy

Supporting Information

Table of Contents

SUPPLEMENTARY FIGURES

A UV-Vis spectra of **3b** (DY-480XL)

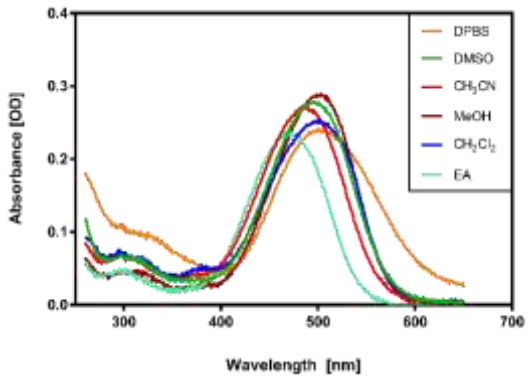

B Fluorescence spectra of **3b** (DY-480XL)

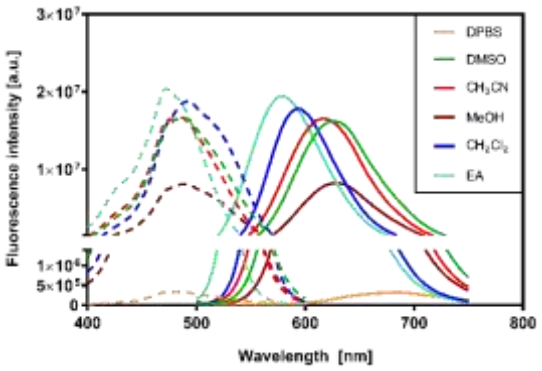

C UV-Vis spectra of **4** (Alexa647)

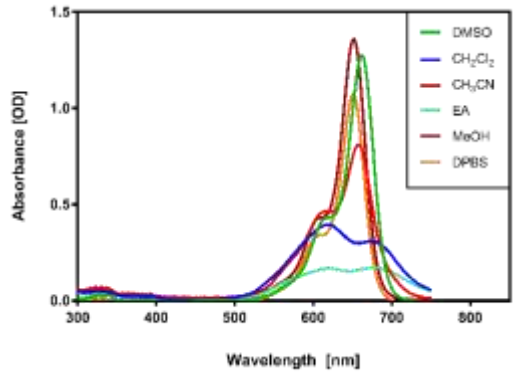

D Fluorescence spectra of **4** (Alexa647)

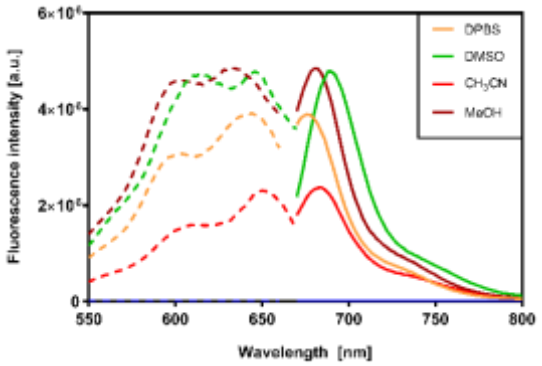

E UV-Vis spectra of **5** (Alexa488)

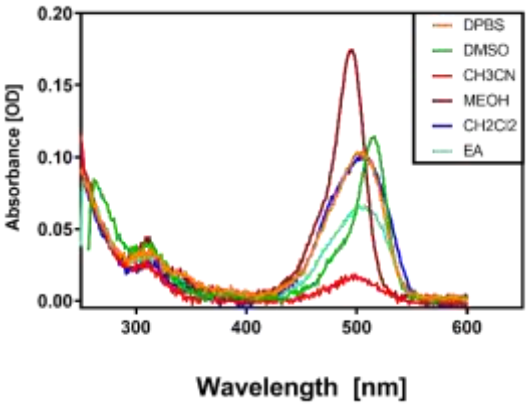

F Fluorescence spectra of **5** (Alexa488)

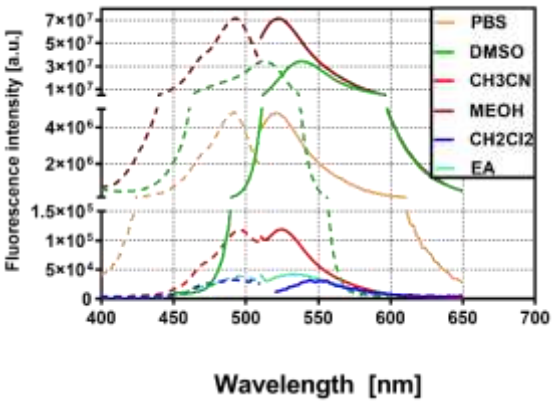

G UV-Vis spectra of **6** (AttoThio12) **H** Fluorescence spectra of **6** (AttoThio12)

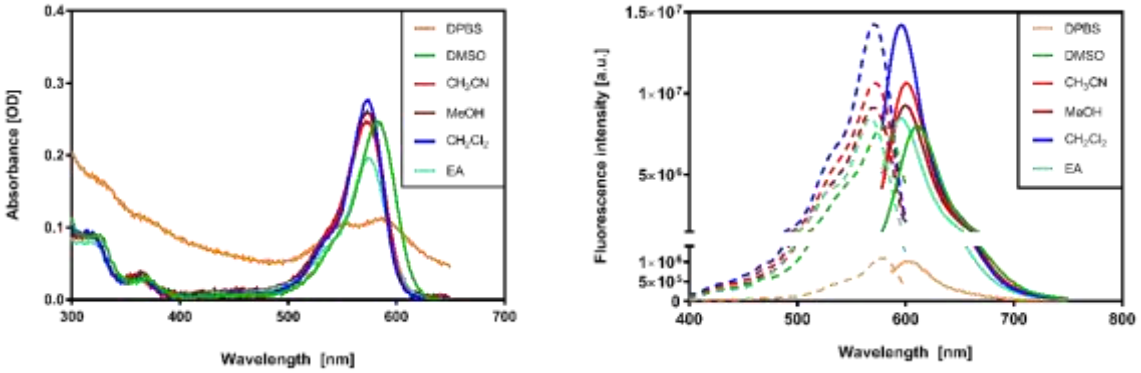

Figure S1. Solution spectra of compound **3b** (DY480-XL) (A and B), **4** (Alexa647) (C and D), **5** (Alexa488) (E and F) and **6** (AttoThio12) (G and H). A/C/E/G) UV-Vis spectra (10 µM compound); B/D/F/H) technical excitation and emission fluorescence spectra not corrected for chromatic aberrations (10 µM compound) in indicated organic solvents (DMSO, methylene chloride (CH_2Cl_2), acetonitrile (CH_3CN), ethyl acetate (EA) and methanol (MeOH) and aqueous solution DPBS (Dulbecco's phosphate buffered saline). Excitation and emission spectra are depicted with dashed or solid lines, respectively.

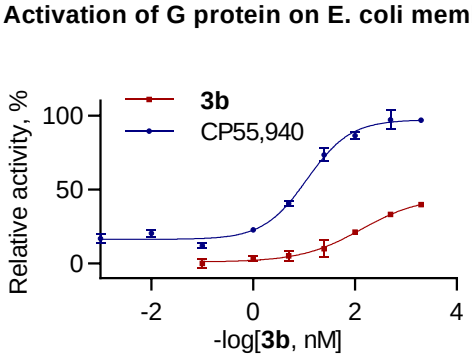

Figure S2. [^{35}S]GTP-γ-S G protein activation assay employing CB_2R on *E. coli* membranes. **3b** EC_{50} = 133 nM, %eff = 44 relative to CP55,940.

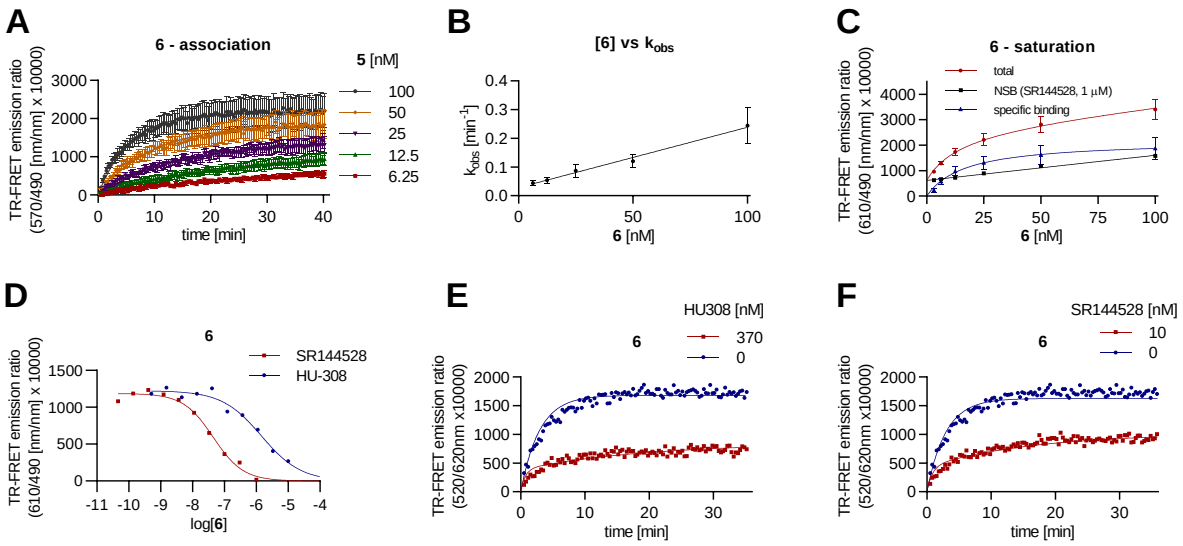

Figure S3. FRET-based fluorescent probe characterization with determination of affinities and binding kinetics of CB_2R compounds. A) Observed association of probe **6** binding to hCB_2R. B) Plot of probe **6** concentration versus observed association rate, k_{obs} increased linearly with fluorescent ligand concentration. C) Saturation analysis showing the binding of probe **6** to hCB_2R. D) Competition association between probe **6** (100 nM) and increasing concentrations of CB_2R specific ligands HU-308 and SR144528 for hCB_2R. Competition association curves of **6** in the presence of E) HU-308 and F) SR144528. All binding reactions were performed in the presence of GppNHp (100 µM) to prevent receptor G protein coupling and the formation of the artificial high-affinity state. Nonspecific-binding levels were determined by inclusion of SR144528 (1 µM). Kinetic and equilibrium data were fitted to the equations described in this Supporting Information to calculate K_d, and k_{on} and k_{off} values for the fluorescent probes; these are summarized in Table 2. Data are presented in mean ± SEM from a representative of 3-5 experiments.

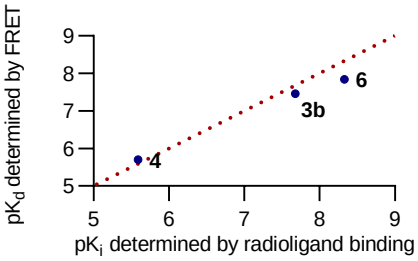

R squared	0.9965
P value	
P (two-tailed)	0.0379

Figure S4. Fluorescent probe binding affinities. Good correlation between pK_d and pK_i values obtained by FRET (HEK293T-Rex SNAP-hCB_2R membranes) and by radioligand assays (hCB_2R-CHO cell membrane preparations) was observed. This suggests that addition of a SNAP-tag to the *N*-terminus of the CB_2R did not affect its pharmacological properties and also validates the FRET binding data showing the usefulness of these probes as fluorescent tracers.

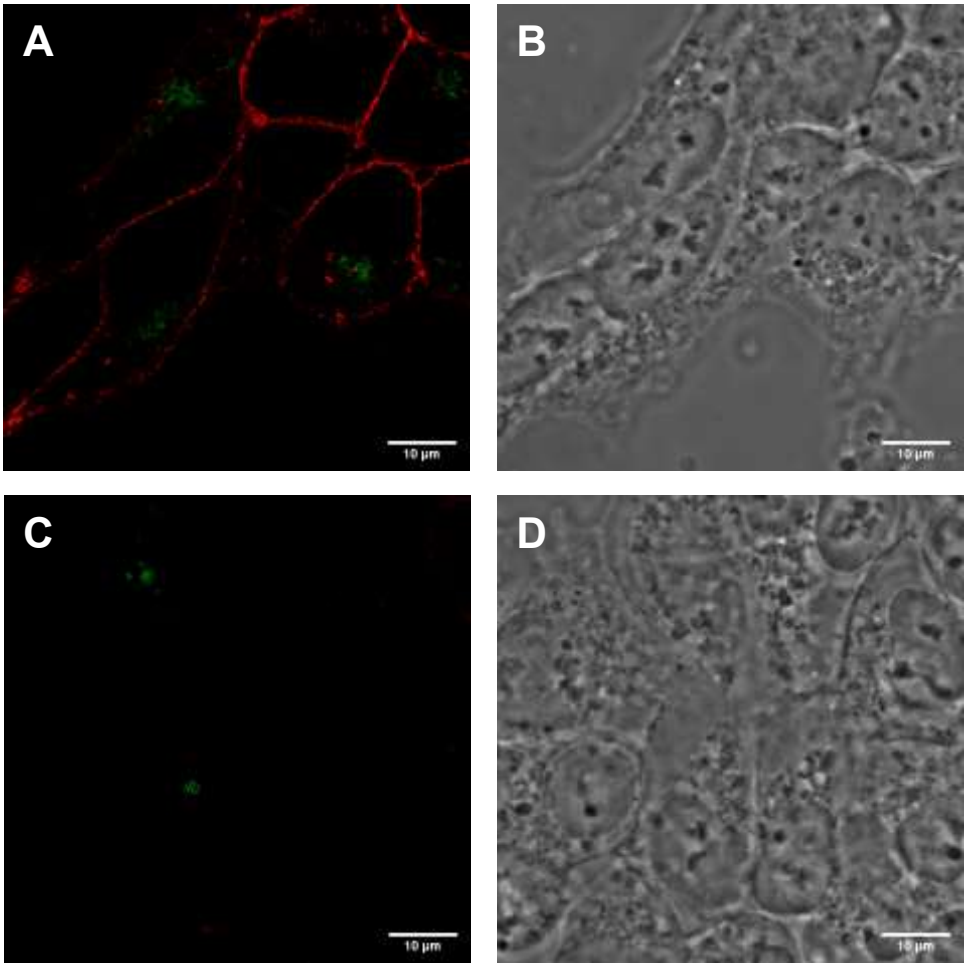

Figure S5. A) Confocal and B) widefield images of N-terminal SNAPtagged-hCB$_2$R expressing T-REx 293 cells labelled with SNAP surface (red) and SNAP cell (green). C) Confocal and D) widefield images of non-expressing T-REx 293 cells depicted processed in the same way. SNAP-hCB$_2$R is almost exclusively expressed on cell membrane. Signal in green channel is comparable in intensity to background.

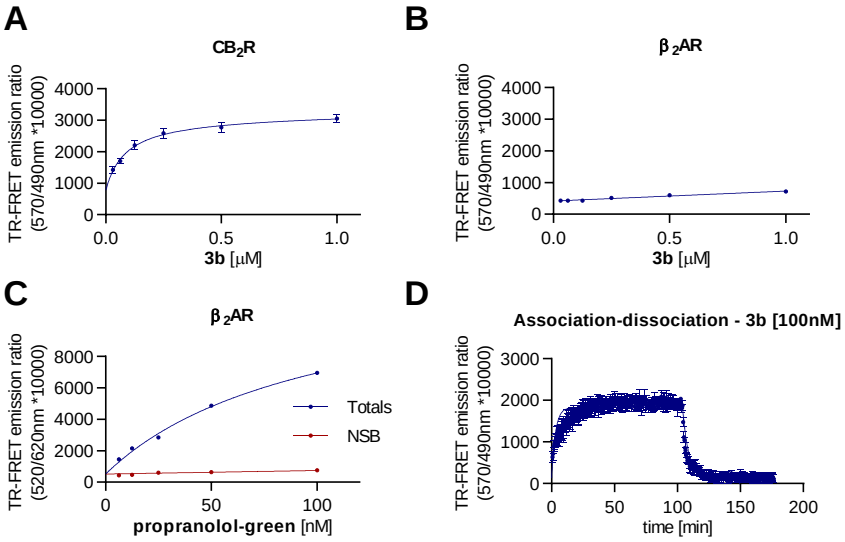

Figure S6. Probe specificity and ligand reversibility demonstrated by TR-FRET binding experiments. A) Total Binding of probe **3b** to HEK-CB$_2$R. Saturation is indicative of specific target binding. B) Total binding of probe **3b** to HEK-β_2AR; linear behavior is indicative of non-specific binding (NSB). C) Binding studies of propranolol green to HEK-β_2AR membranes. D) Association-dissociation experiments for **3b** in which HU-308 (10 μM) added at 100 min results in full dissociation of the probe.

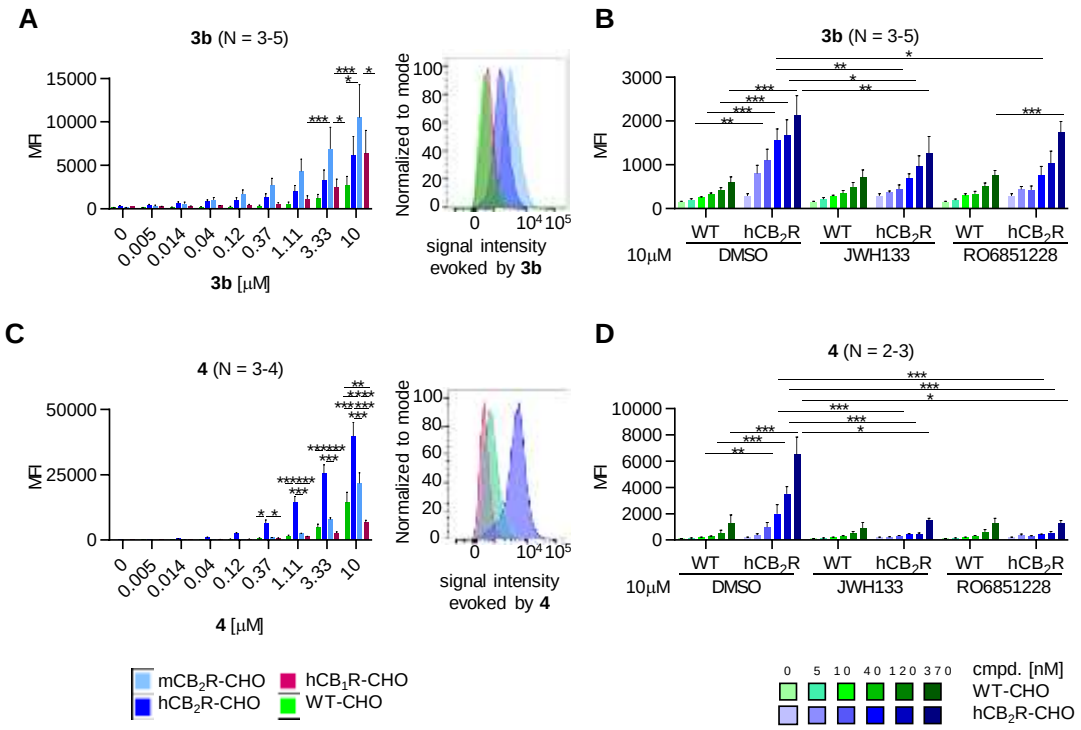

Figure S7. A/C) FACS analysis of cells incubated with fluorescent probes at varying concentrations. Representative fluorescent intensity histograms of cells incubated with 0.37 μM fluoroprobe. Mean ± SEM Two-way ANOVA followed by Bonferroni post hoc analysis, * p<0.05; ** p<0.01; *** p<0.005. B/D) FACS analysis of cells pre-treated with 10 μM of competitor ligands and subsequently stained with varying concentrations of fluoroprobe. Mean ± SEM, Two-way ANOVA followed by Bonferroni post hoc analysis, * p<0.05; ** p<0.01; *** p< 0.005.

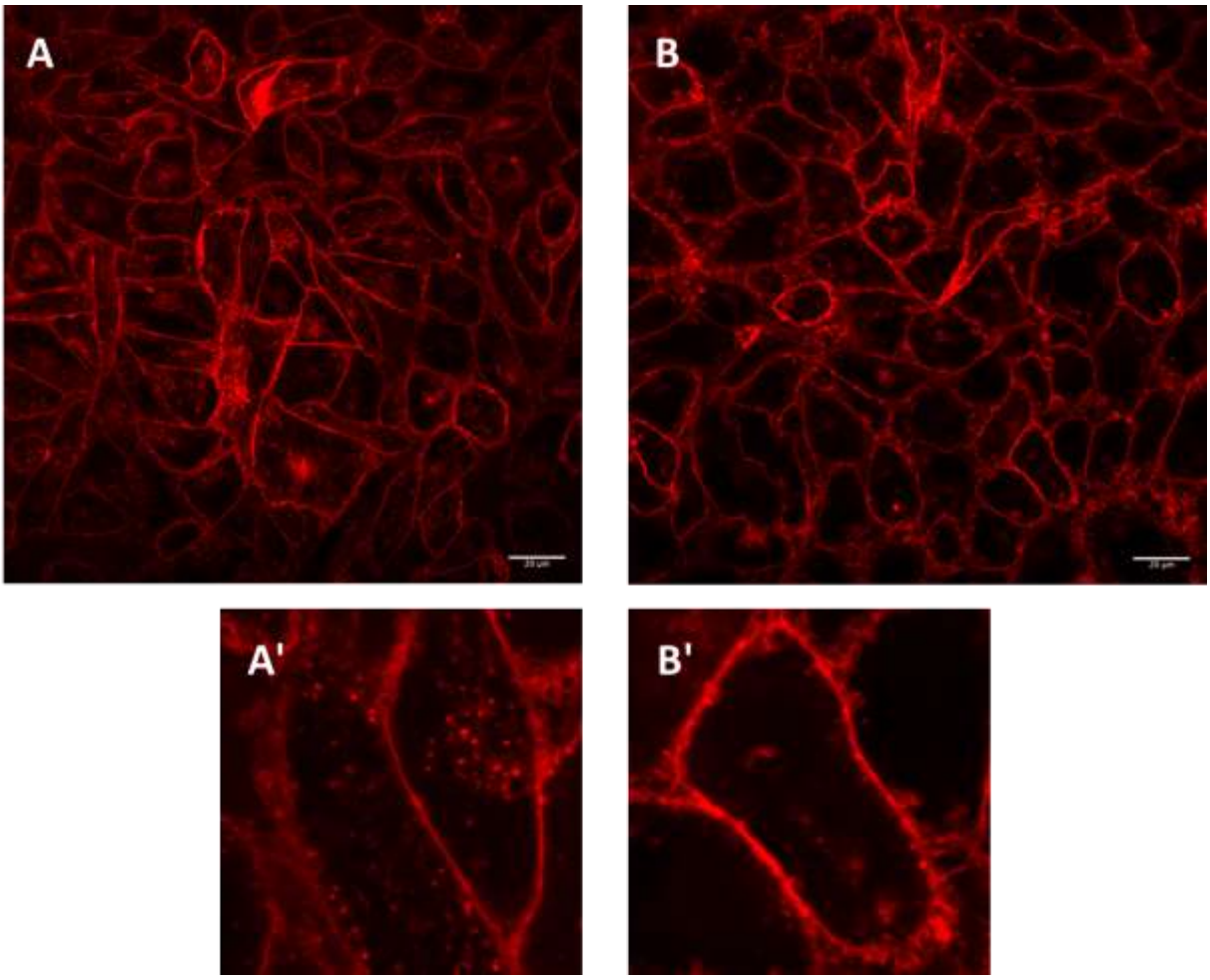

Figure S8. A) Airyscan high-resolution imaging of CHO cells overexpressing hCB_2R incubated with 0.2 μM **3b**. B) Co-incubation with endocytosis inhibitors reduces level of fluorescent probe internalization. Pictures showed cells incubated for 1 h with **3b** in the absence (A and A') and in the presence (B and B') of endocytosis inhibitors (i.e. 400 mM sucrose and 5 μg/mL filipin). In the presence of sucrose and filipin, the reduction of hCB_2R receptor endocytosis was almost complete, as shown by the robust decrease in punctate vesicles within the cells (see magnified regions shown in panels A'/B').

SUPPLEMENTARY TABLES

Table **S1**. Fluorescence excitation and emission wavelengths for CB_2R-selective fluorescent ligands (10 μM) with corresponding fluorescence intensities and Stokes shifts recorded in various solvents.

Probe	Fluorescence data	DPBS	DMSO	CH_3CN	MeOH	CH_2Cl_2	EA
3b (DY-480XL)	Excitation λ [nm]	486	486	484	490	492	472
	Emission λ [nm]	684	626	616	628	594	578
	Stokes shift [nm]	198	140	132	138	102	106
	Signal intensity • 10^6 [a.u.][a]	0.3[b]	16.7	16.7	8.1	18.8	20.4
4 (Alexa647)	Excitation λ [nm]	648	648	648	632	*nt*	*nt*
	Emission λ [nm]	680	689	689	680	*nt*	*nt*
	Stokes shift [nm]	32	41	41	48	*na*	*na*
	Signal intensity • 10^6 [a.u.]	3.8	4.7	2.3	4.9	*nt*	*nt*
5 (Alexa488)	Excitation λ [nm]	492	512	496	492	492	496
	Emission λ [nm]	522	538	524	522	544	532
	Stokes shift [nm]	30	26	28	30	52	36
	Signal intensity • 10^6 [a.u.]	4.8	34.3	1.2	71.5	0.3	0.4
6 (AttoThio12)	Excitation λ [nm]	576	578	578	570	570	568
	Emission λ [nm]	600	610	600	600	596	596
	Stokes shift [nm]	24	32	22	30	26	28
	Signal intensity • 10^6 [a.u.]	1.0	8.0	10.6	9.1	14.2	8.5

[a] a.u. – arbitrary units [b] limited solubility in DPBS, measured at 1.0 μM in presence of 0.1% (v/v) DMSO; nt: not tested; na: not applicable

Discussion of Results

As expected, the fluorescence intensity observed for compounds **3b** (DY-480XL) and for **6** (AttoThio12) increased with decreasing dielectric constant of the solvents: aqueous solution (PBS, ε_{25} = 79.0) < dimethyl sulfoxide (DMSO, ε_{20} = 47) < acetonitrile (CH_3CN, ε_{20} = 36.64) ≤ methanol (MeOH, ε_{25} = 32.6) < methylene chloride (CH_2Cl_2, ε_{20} = 9.08) ≤ ethyl acetate (EA, ε_{25} = 6).[1],[2] Consequently, the fluorescence intensity is expected to increase when in close proximity of the cell membrane (ε = 3) or when bound to the hydrophobic binding site of CB_2R. The lower fluorescence intensity values observed for **3b** (DY-480XL) and **6** (AttoThio12) in methanol (MeOH) and ethyl acetate (EA), respectively, may indicate specific solvent effects, but overall the expected trend of increasing of fluorescence signal intensity with decrement of solvent polarity is observed.

3b (DY-480XL). The fluorescence excitation and emission maxima were observed at wavelengths ranging from 472 - 490 nm and 594 - 684 nm, respectively, depending on the applied solvent. The highest fluorescence emission signal was observed in ethyl acetate (Fig.

S1 and Table S1). The lowest fluorescence signal was observed in aqueous solution (DPBS). An increasing redshift of the fluorescence emission maxima with increasing solvent polarity was observed, with the highest shift (106 nm) monitored for aqueous solution DPBS when compared to ethyl acetate. The Stokes shift was found to be relatively high with the lowest value of 102 nm observed in methylene chloride and the highest shift value of 198 nm observed in DPBS.

4 (Alexa647). The fluorescence excitation and emission maxima were observed at wavelengths ranging from 632 - 648 nm and 680 - 689 nm, respectively, depending on the applied solvent. The highest fluorescence emission signal was observed in methanol and DMSO (Fig. S1 and Table S1). The lowest fluorescence signal was observed in acetonitrile. The Stokes shift was observed to be between 32 nm in phosphate buffer and 48 nm in methanol.

5 (Alexa488). The fluorescence excitation and emission maxima were observed at wavelengths ranging from 492 - 512 nm and 522 - 544 nm, respectively, depending on the applied solvent. The highest fluorescence emission signal was observed in methanol (Fig. S1 and Table S1). The lowest fluorescence signal was observed in methylene chloride. The Stokes shift was observed to be between 26 nm in DMSO and 52 nm in methylene chloride.

6 (AttoThio12). The fluorescence excitation and emission maxima were observed at wavelengths ranging from 570 - 578 nm and 596 - 610 nm, respectively, depending on the applied solvent. The highest fluorescence emission signal was observed in methylene chloride (Fig. S1 and Table S1). The lowest fluorescence signal was observed in ethyl acetate. The Stokes shift was observed to be 22 nm in acetonitrile and 32 nm in DMSO.

Table S2. Evaluation of **3b** off-target activity via screening against a representative set of common off-targets (Eurofins).[3] Data shown is the mean percentage of inhibition for binding assays and the mean percentage of inhibition for enzyme and cell-based assays at a test concentration of 10 µM (n=2).

ASSAY NAME	RESPONSE/READOUT	VALUE
MAO-A (h)	Enzymatic activity	-1.5
5-HT transporter (h) (antagonist radioligand)	Specific binding	-1.0
5-HT_{1A} (h) (agonist radioligand)	Specific binding	7.0
5-HT_{2A} (h) (agonist radioligand)	Specific binding	-1.6
5-HT_{2B} (h) (agonist radioligand)	Specific binding	39.0
5-HT_3 (h) (antagonist radioligand)	Specific binding	3.9
A_1 (h) (agonist radioligand)	Specific binding	6.1
A_3 (h) (agonist radioligand)	Specific binding	12.3
Abl kinase (h)	Enzymatic activity	-5.0
ACE (h)	Enzymatic activity	-15.0
acetylcholinesterase (h)	Enzymatic activity	4.1
α_{1A} (h) (antagonist radioligand)	Specific binding	3.5
α_{2A} (h) (antagonist radioligand)	Specific binding	-5.6
AR (h) (agonist radioligand)	Specific binding	17.3
AT_1 (h) (antagonist radioligand)	Specific binding	-4.0
β_1 (h) (agonist radioligand)	Specific binding	13.0
β_2 (h) (antagonist radioligand)	Specific binding	-6.2
BZD (central) (agonist radioligand)	Specific binding	-8.5
Ca^{2+} channel (L, diltiazem site) (benzothiazepines) (antagonist radioligand)	Specific binding	-17.8
CB_1R (h) (agonist radioligand)	Specific binding	35.3
CCK_1 (CCK_A) (h) (agonist radioligand)	Specific binding	7.5
CDK_2 (h) (cycA)	Enzymatic activity	7.1
Cl^- channel (GABA-gated) (antagonist radioligand)	Specific binding	51.3
COX2(h)	Enzymatic activity	36.9
D_1 (h) (antagonist radioligand)	Specific binding	12.8
D_{2S} (h) (agonist radioligand)	Specific binding	3.6
ERα (h) (agonist radioligand)	Specific binding	-1.4
FP (h) (agonist radioligand)	Specific binding	74.0
glycine (strychnine-insensitive) (antagonist radioligand)	Specific binding	33.9
GR (h) (agonist radioligand)	Specific binding	0.5
GSK3α (h)	Enzymatic activity	6.7
GSK3β (h)	Enzymatic activity	2.8

H_1 (h) (antagonist radioligand)	Specific binding	-3.1
H_2 (h) (antagonist radioligand)	Specific binding	-11.0
H_3 (h) (agonist radioligand)	Specific binding	29.4
HIV-1 protease	Enzymatic activity	14.3
κ (KOP) (agonist radioligand)	Specific binding	22.3
M_1 (h) (antagonist radioligand)	Specific binding	25.5
M_2 (h) (antagonist radioligand)	Specific binding	12.9
MMP-9 (h)	Enzymatic activity	12.2
μ (MOP) (h) (agonist radioligand)	Specific binding	-2.8
N muscle-type (h) (antagonist radioligand)	Specific binding	-12.6
N neuronal $\alpha_4\beta_2$ (h) (agonist radioligand)	Specific binding	3.9
norepinephrine transporter (h) (antagonist radioligand)	Specific binding	-1.7
PCP (antagonist radioligand)	Specific binding	-3.4
PDE3B (h)	Enzymatic activity	21.4
PDE4D2 (h)	Enzymatic activity	13.9
PPARγ (h) (agonist radioligand)	Specific binding	10.8
xanthine oxidase/ superoxide O2- scavenging	Enzymatic activity	6.4
ZAP70 kinase (h)	Enzymatic activity	5.1

Table S3. Calculated *n*-octanol-water partition coefficients (AlogP)[4] for fluorescent probes **2** – **5**.

Compound	MW	AlogP	HAC[a]
2	885.1	8.7	64
3a	910.2	11.5	65
3b	951.2	11.6	68
4	1367.8	12.0	93
5	1084.3	7.9	76
6	939.3	10.9	68

[a] HAC heavy atom count

MOLECULAR DOCKING

The X-ray structures of CB_2R complexed with antagonist AM10257 (5zty) and agonist WIN 55,212-2 (6PT0) were used as template to dock CB_2R ligands. The docking experiments were performed with the software GOLD[5] (Chemical Computing Group) with default settings. The best 10 docking poses for each compound were energy-minimized within the binding pocket using MOE (CCG, Montreal)[6] and examined visually to select the most reasonable docking mode with respect to molecular interactions and internal conformational strain. The final selection was based on checking consistency with the available structure-activity relationship information.

IN VITRO PHARMACOLOGY

Radioligand binding assay and cAMP assay

Radioligand binding assays and forskolin-stimulated cAMP assays were performed as described by Soethoudt et al.[7] The CB_2R-expressing cell lines are clonal and the B_{max} of cell lines is indicated in brackets. WT-CHO, hCB_2R -CHO (2.08 pmol/mg protein) and hCB_1R-CHO (5.5 pmol/mg protein) were produced in house and mCB_2R-CHO cells (11.8 pmol/mg protein) have the following reference (PathHunter® CHO-K1 mCNR2 (CB_2R) β-Arrestin Cell Line DiscoverX, 93-0472C2). Cells were cultured and membranes for radioligand binding assays prepared in analogy to Soethoudt et al.[7] Reference compounds for binding and cAMP assays were selected in accordance to literature.[7] The corresponding mean K_i and EC_{50} values, as well as standard error of the mean (SEM), are stated below. Data are means from one or two independent experiments performed in triplicate.

hCB_2R K_i

The mean K_i value of the positive control JWH133 used for each run was 34.9 nM, with standard error of the mean (SEM) of ±3.4 nM (n=128).

hCB_1R K_i

The mean Ki value of the positive control Rimonabant used for each run was 2.8 nM, with standard error of the mean (SEM) ±0.2 nM (n=105).

mCB_2R K_i

The mean Ki value of the positive control WIN55212-2 used for each run was 5.8 nM, with standard error of the mean (SEM) ±1.3 nM (n=57).

hCB_2R, mCB_2R and hCB_1R cAMP EC_{50}

The mean EC_{50} value of the positive control CP55,940 used for each run were 0.08 nM, 0.05 nM and 0.11 nM, respectively, with respective standard errors of the mean (SEM) ±0.011 nM (n=114), ±0.007 nM (n=94) and ±0.013 nM (n=95).

Passive membrane permeability assay (PAMPA)

The parallel artificial membrane permeability assay is a method which determines the permeability of substances from a donor compartment, through a lipid-infused artificial membrane into an acceptor compartment.[8] The read-out is a permeation coefficient P_{eff} drug as well as test compound concentrations in donor, membrane and acceptor compartments. A 96-well microtiter plate completely filled with aqueous buffer solutions (pH 7.4/ 6.5) is covered with a microtiter filterplate in a sandwich construction. The hydrophobic filter material (Durapore/Millipore; pore size 0.22–0.45 μm) of the first 48 wells (sample) of the filterplate is impregnated with a 1–20% solution of lecithin in an organic solvent (dodecane, hexadecane, 1,9-decadiene). The filter surface of the remaining 48 wells (reference) is wetted with a small volume (4–5 μL) of a 50% (v/v) methanol/buffer solution. Transport studies were started by the transfer of 100–200 μL of a 250 or 500 μM stock solution on top of the filter plate in the sample and in the reference section, respectively. In general 0.05 M TRIS, pH 7.4, or 0.05 M phosphate, pH 6.5, buffers were used. The maximum DMSO content of the stock solutions was 5%.

FLUORESCENCE SPECTROSCOPY

Material and methods

UV/Vis absorbance spectra of 50 µM solutions of fluorescent probes in various solvents were recorded in a wavelength range of 250-750 nm to determine λ_{max} used later for compound excitation (1 cm path length, room temperature, scan step 1 nm; Thermo Evolution 600 UV/Vis spectrophotometer, Thermo Electron Scientific Instruments LLC, Madison, WI, USA). Due to the limited solubility of the probes in DPBS, the spectra in DPBS were measured in a cuvette with 10 cm path length at 5 µM in presence of 0.1 % (v/v) DMSO.

Technical excitation and emission fluorescence spectra (uncorrected for chromatic aberrations) of fluorescent probes were measured at 10 µM compound concentration (20°C, integration time 1s, scan step 2 nm, slits 2.4 mm and 2 mm in excitation and emission, respectively; ISS Inc. PC1 fluorometer, Champaign, IL, USA) in organic (dimethyl sulfoxide (DMSO), methylene chloride (CH_2Cl_2), acetonitrile (CH_3CN), ethyl acetate (EA) and methanol (MeOH) and aqueous solvent (Dulbecco's phosphate buffered saline, DPBS). Due to the limited solubility of the HU-308-based probes in DPBS, the spectra in DPBS were measured at 1.0 µM in the presence of 0.1% (v/v) DMSO and then scaled to expected fluorescence signal intensity at concentration of 10 µM by multiplication of the signal intensity by factor of 10.

TR-FRET KINETIC CB_2R BINDING ASSAY

Cell Culture

Cells were maintained in a humidified environment at 37 °C and 5% CO_2 in Dulbecco's modified Eagle's medium (DMEM) with 10% fetal bovine serum (FBS) containing blasticidin (5 μg/ml; Invitrogen) and (Zeocin; 20 μg/mL; Invitrogen). For inducible expression, SNAP-tagged human CB_2R receptor cDNAs, in pcDNA4/TO were introduced through transfection, using PEI into HEK293T-Rex cells (Invitrogen, which express Tetracyclin repressor protein to allow inducible expression). A mixed population stable line was selected by resistance to blasticidin (TR vector, 5 μg/mL) and Zeocin; (receptor plasmid, 20 μg/mL). For receptor-inducible expression, cells were seeded into 175 cm^2 flasks, grown to 70% confluence and DMEM containing 1 μg/mL tetracycline added. 24h later cells were labelled with SNAP-Lumi4-Tb (CisBio) and membranes prepared as described in detail below.

Terbium labeling of SNAP-tagged CB_2R HEK293-TR cells

Cell culture medium was removed from the 175 cm^2 flasks containing confluent adherent CB_2R HEK293T-Rex cells. Cells were washed 1× in PBS (GIBCO Carlsbad, CA) followed by 1x Tag-lite labeling medium (LABMED, CisBio) to remove the excess cell culture media, then ten milliliter of LABMED containing 100 nM of SNAP-Lumi4-Tb was added to the flask and incubated for 1 h at 37 °C under 5% CO_2. Cells were washed 1× in PBS (GIBCO Carlsbad, CA) to remove the excess of SNAP-Lumi4-Tb then detached using 5 ml of GIBCO enzyme-free Hank's-based cell dissociation buffer (GIBCO, Carlsbad, CA) and collected in a vial containing 5 mL of DMEM (Sigma-Aldrich) supplemented with 10% fetal calf serum. Cells were pelleted by centrifugation (5 min at 1500 rpm) and the pellets were frozen to −80 °C. To prepare membranes, homogenization steps were conducted at 4 °C (to avoid receptor degradation) as described in Klein-Herenbrink et al., 2016.[9] Total protein concentration of the membrane preparation was measured using BCA assay (Pierce).

Fluorescent ligand-binding assays

All fluorescent ligand binding experiments were conducted in white 384-well Optiplate plates (PerkinElmer), in assay binding buffer, LABMED containing 5 mM HEPES, 0.5% BSA, 0.02% pluronic acid pH 7.4, and 100 μM GppNHp.

The stable GTP analogue, GppNHp was included to promote a single population of receptors (free of G protein) since the original Motulsky-Mahan model[10] can only be applied under such stringent conditions with probe and compounds competing for a single receptor species. Previous radioligand binding data has suggested the presence of a high affinity population of

effector bound receptors.[11] The resulting model fits obtained with the fluorescent probes are consistent with the presence of a single population of low affinity receptors. In all cases, nonspecific binding was determined by the presence of 1 μM SR144528.

Determination of fluorescent ligand binding kinetics and equilibrium affinity

To accurately determine association rate (k_{on}) and dissociation rate (k_{off}) values, the observed rate of association (k_{ob}) was calculated using at least five different concentrations fluorescent ligand. The appropriate concentration of fluorescent ligand binding was incubated with human CB_2R cell membranes (4 μg total protein per well) in assay binding buffer (final assay volume, 40 μL). The degree of fluorescent ligand bound to the receptor was assessed at multiple time points by HTRF detection to allow construction of association kinetic curves. The resulting data were globally fitted to the association kinetic model (Eq. 1) to derive a single best-fit estimate for k_{on} and k_{off} as described under data analysis. Saturation analysis was performed at equilibrium, by simultaneously fitting total and Nonspecific (NSB) binding data (Eq. 3) allowed the determination of fluorescent ligand binding affinity.

Determination of ligand binding kinetics

To determine the association and dissociation rates of CB_2R specific ligands, we used a competition-association binding assay.[10] This approach involves the simultaneous addition of both fluorescent ligand and competitor to the receptor preparation so that at t = 0 all receptors are unoccupied. To achieve this aim HEK293 cell membranes containing the human CB_2R (4 μg per well) were added to wells containing 100 nM **3b** or **6**, a concentration which avoids ligand depletion in this assay volume, and a fixed concentration of the antagonist SR144528 or the agonist HU-308, designed to produce approximately 50% inhibition of probe binding, in a total assay volume of 40 μL. The degree of fluorescent ligand bound to the receptor was assessed at multiple time points by HTRF detection.

The kinetic parameters of the fluorescent ligands **3b** and **6** plus those of unlabeled compounds were determined using a start time of ~30 sec and an interval time of 20 sec. Non-specific binding was determined as the amount of TR-FRET signal detected in the presence of SR144528 (1μM) and was subtracted from each time point, meaning that t = 0 was always equal to zero. Each time point was conducted on the same 384-well plate incubated at room temperature with orbital mixing (1sec of 100 RPM/cycle). Data were globally fitted using (Eq. 2) to simultaneously calculate k_{on} and k_{off} of unlabeled compounds.

Competition binding

To determine the affinity of CB_2R specific ligands, we used a simple competition kinetic binding assay. This approach involves the simultaneous addition of both fluorescent ligand and competitor to the CB_2R preparation. 100 nM **3b** and **6**, concentrations which avoid ligand depletion in this assay volume, were added simultaneously with increasing concentrations of the unlabeled compound to CB_2R cell membranes (4 µg total protein per well) in 40 µl of assay buffer in a 384-well plate incubated at ambient temperature with orbital mixing. The degree of fluorescent ligand bound to the receptor was assessed at equilibrium by HTRF detection. Nonspecific binding was determined as the amount of HTRF signal detected in the presence of SR144528 (1 µM) and was subtracted from total binding, to calculate specific binding for construction of IC_{50} curves and calculation of affinity values (Eq. 4 and 5).

Signal detection and data analysis

Signal detection was performed on a Pherastar FSX (BMG Labtech, Offenburg, Germany). The terbium donor was always excited with eight laser flashes at a wavelength of 337 nm. TR-FRET signals were collected at both at 570 (acceptor) and 490 nm (donor), when using the DY480XL-based fluorescent ligand **3b** and at 665 (acceptor) and 620 nm (donor), when using the red acceptor fluorescent ligand **4**. The AttoThio12-based fluorescent ligand, **6** required production of a custom manufactured modules with emissions measured at 610 (acceptor) and 490nm (donor) respectively. HTRF ratios were obtained by dividing the acceptor signal by the donor signal and multiplying this value by 10’000. All experiments were analyzed by non-linear regression using Prism 8.0 (GraphPad Software, San Diego, USA).

Fluorescent ligand association data were fitted as follows to a global fitting model using GraphPad Prism 8.0 to simultaneously calculate k_{on} and k_{off} using the following equation,

$$k_{ob} = [L]^*k_{on} + k_{off} \qquad \text{(Eq. 1)}$$

$$Y = Y_{max}^*(1-\exp(-1^*k_{ob}^*X))$$

Where, k_{ob} equals the observed rate of ligand association and k_{on} and k_{off} are the association and dissociation-rate constants respectively of the fluorescent ligand. In this globally fitted model of tracer binding, tracer concentrations [L] are fixed, k_{on} and k_{off} are shared parameters whilst k_{obs} is allowed to vary. Here, Y is the level of receptor-bound tracer, Y_{max} is the level of tracer binding at equilibrium, X is in units of time (eg. min) and k_{obs} is the rate in which equilibrium is approached (eg. min^{-1}).

Association and dissociation rates for unlabeled antagonists were calculated using the following equations first described by Motulsky and Mahan.[10]

$$K_A = k_1[L] + k_2$$

$$K_B = k_3[I] + k_4$$

$$S = \sqrt{((K_A - K_A)^2 + 4 \cdot k_1 \cdot k_3 \cdot L \cdot I \cdot 10^{-18})}$$

$$K_F = 0.5 * (K_A + K_B + S)$$

$$K_S = 0.5 * (K_A + K_B - S)$$

$$Q = \frac{B_{max} * K_1 * L * 10^{-9}}{K_F - K_S}$$

$$Y = Q \cdot \left(\frac{k_4 \cdot (K_F - K_S)}{K_F \cdot K_S} + \frac{k_4 - K_F}{K_F} exp^{(-K_F \cdot X)} - \frac{k_4 \quad K_S}{K_S} exp^{(-K_S \cdot X)}\right) \qquad \text{(Eq. 2)}$$

Where: X = Time (min), Y = Specific binding (eg. CPM or HTRF units eg. HTRF ratio 520nm/620nm x 10'000), k_1 = k_{on} tracer (M^{-1} min^{-1}), k_2 = k_{off} tracer (min^{-1}), L = Concentration of tracer used (nM), I = Concentration unlabeled ligand (nM). Fixing the above parameters allows the following to be calculated: k_3 = Association-rate constant of unlabeled ligand (M^{-1} min^{-1}), k_4 = Dissociation-rate constant of unlabeled ligand (min^{-1}), B_{max} = Maximal specific binding of the system at equilibrium binding (eg. CPM or HTRF units, eg. HTRF ratio 520nm/620nm x 10'000).

Saturation binding data were analysed by non-linear regression according to a one-site equation by globally fitting total and NSB. Individual estimates for the fluorescent ligand dissociation constant (K_d) were calculated using the following equations where L is the fluorescent ligand concentration:

$$\text{Total binding} = \text{Specific} + NSB = \frac{\text{Bmax} * [\text{L}]}{Kd + [L]} + \text{slope} * [\text{L}] + Background$$

$$\text{NSB} = \text{slope} * [\text{L}] + Background$$

(Eq. 3)

Fitting the total and NSB data sets globally (simultaneously), sharing the value of slope, provides one best-fit value for both the K_d and the B_{max}.

Competition displacement binding data were fitted to sigmoidal (variable slope) curves using a 'four-parameter logistic equation':

$$Y = \text{Bottom} + (\text{Top}-\text{Bottom})/(1+10^{(\log IC50-X).\text{Hill coefficient}}) \quad \text{(Eq. 4)}$$

IC_{50} values obtained from the inhibition curves were converted to K_i values using the method of Cheng and Prusoff.[12]

$$K_i = IC_{50}/(1+[\text{fluorescent tracer concentration}]/K_d) \quad \text{(Eq. 5)}$$

SNAP-hCB$_2$R Construct: Localization Studies

A 6-well Costar cell culture plate (Corning) containing 18 mm square no 1.0 coverslips was poly-D-lysine coated. T-REx 293 cells, containing SNAP-tagged hCB$_2$R on a pcDNA4/TO vector, were seeded at a density of 600 000/well in growth medium (DMEM high glucose (Sigma-Aldrich) with 10% FBS, 20 ug/mL Zeocin, 15 ug/mL Blasticidin). After 7 h, CB$_2$ expression was induced using 1 μg/mL tetracycline. The cells were stained with SNAP dyes 24 h after induction: First, cells were incubated for 30 min with 200 nM SNAP-surface 647 (New England Biolabs), washed 3x 5 min in growth medium to remove non-reacted dye. Secondly, the cells were stained with 200 nM SNAP-cell Oregon Green (New England Biolabs) for 30 min and washed 3 x 5 min in growth medium to remove non-reacted dye. The cells were incubated for 30 min in growth medium to enable non-reacted dye to diffuse out of the cells. Lastly, they were washed for 3 x 5 min washes in PBS and fixed with 3% PFA. The coverslip was mounted in vectashield anti-fade mounting medium (Vector Laboratories).

Cells were imaged using a Zeiss LSM 710 laser scanning confocal microscope fitted with a Zeiss Plan-Apochromat 63x/1.40 NA oil immersion objective. A Helium Neon 633 nm laser and Argon laser at 488 were used to excite the Alexafluor 647 and Alexafluor 488 fluorophores respectively and emission was collected using a 488/561/633 multi beam splitting filter. Images were taken at 512 × 512 pixels per frame with line average of 4 and a slice of 53.36 um for confocal images. Laser power and gain were kept constant between experiments.

FACS ANALYSIS

CHO cells

For validation of CB_2R-fluoroprobes via FACS analysis, 50'000 WT-CHO, or CHO cells overexpressing hCB_2R, mCB2R or hCB_1R were incubated with different concentrations of CB_2R-fluoroprobes (0.005 µM-10 µM) in PBS/0.5%BSA/2 mM EDTA for 30 min at 4 °C. For cold ligand replacement experiments, 50'000 WT-CHO cells or CHO cells overexpressing hCB_2R were pre-incubated with 10 µM JWH133 or RO6851228 in PBS/0.5%BSA/2 mM EDTA at room temperature. After 30 min, different concentrations of CB_2R-fluoroprobes were added to the cell suspensions (5 nM-370 nM) and cells were incubated for another 30 min at 4 °C. After CB_2R-fluoroprobe incubation, cells in both experiments were washed 3 times with PBS/0.5%BSA/2 mM EDTA and resuspended in PBS/0.5%BSA/2 mM EDTA containing 1:1000 AquaZombie (Biolegend 423102). FACS analysis was performed on BD Fortessa. After exclusion of dead cells, mean fluorescent intensity of viable cells was determined.

Mouse Microglia Cells

Microglial isolation: After perfusion with ice-cold PBS, brains of male mice (5xFAD or 5xFAD/CB_2KO)[13] were dissected and enzymatically digested using trypsin-EDTA for 40 min at 37 °C and re-suspended in DMEM, and then filtered with a 70 μm cell strainer. Microglia and infiltrating mononuclear cells were isolated at the interface of 70% and 30% Percoll (after centrifugation 2800 g for 20 minutes).

After isolation of microglial cells, BSA 1%/PBS was used as blocking solution by incubation at 4 °C for 30 min. Cells were then stained with **3b** (DY-480XL) probe at 1.5, 3, 4.5 and 6 μM and labeled with anti-CD11b-phycoerythrin (PE) and anti-CD45-allophycocyanin-Vio770 (APC-Vio770) at 4 °C for 30 min. Cells were washed with PBS and re-suspended in 400 μL of PBS.

Cytometry analysis: Isolated microglia and infiltrating mononuclear cells were stained and analyzed by flow cytometry (MACS-Quant) after gating live cells based on FSC and SSC. Cell doublets were excluded in FSC-A/FSC-W panel. The expression of CD45 and CD11b was measured to distinguish CNS-resident CD45lo microglia from infiltrating CD45hi leukocytes, in conjunction with their expression of CD11b (macrophages) or lack thereof (lymphocytes). Quantification of **3b** (DY-480XL)-positive microglia was then performed.

TIME-LAPSE CONFOCAL IMAGING

In order to minimize receptor internalization and thus to maximize the fluorescence signal on the plasma membrane, these experiments were performed at 22 °C. For real-time labeling studies, cells were plated onto 8-well chamber slides (Ibidi, Milan, Italy), at a density of 50'000 cells/well and cultured for 24 h. For a nuclear staining, the medium was replaced by 1 µg/mL Hoechst 33342 in RPMI (Sigma-Aldrich, Milan, Italy) and the cells were incubated for 10 minutes at 37 °C, then washed with PBS twice. A small volume of the **3b**, dissolved at 10 mM in DMSO, was mixed with the 20% (w/v) Pluronic F-127 in DMSO (Sigma-Aldrich) at a ratio of 1:1, immediately before use. To inhibit clathrin- and caveolae-dependent endocytosis, we pretreated the cells for 30 min with 400 mM sucrose and 5 µg/mL filipin.[14] Prior to imaging, the solution of compound **3b** and Pluronic F-127 was diluted at 0.2 µM in HEPES-buffered RPMI and quickly added to the cells without any washing step during the time-lapse experiments. Imaging was performed by using confocal laser scanning microscope ZEISS LSM 800 equipped with an Airyscan detection unit (Zeiss, Oberkochen, Germany). To maximize the resolution enhancement, a high numerical aperture oil immersion alpha Plan-Apochromat 63X/1.40 oil DIC M27 objective was used. **3b** was excited using a 488 nm laser line and the corresponding fluorescence emission was detected using a 655 nm long-pass filter, whereas Hoechst 33342 was excited with a dedicated 405 nm UV diode, and the corresponding fluorescence emission was detected using a 490/40 nm band-pass filter. Images within each experiment were collected by using identical laser-power, offset, and gain setting that was adjusted to minimize the level of auto-fluorescence. Live imaging was performed at 22 ± 2°C by recording one frame every 15 sec for 10 min. At the end of recording session, living cells were imaged with Airyscan mode. Each image was taken at the equatorial plan of the cells, using the ZEN Blue 2.3 software (Zeiss). Super-resolution image processing was performed using the Airyscan processing toolbox in the ZEN software. The data were exported as TIFF files and analyzed using the Fiji software (National Institutes of Health; https://imagej.net/Fiji). A Gaussian kernel filter was applied to the images using a standard deviation of 0.8 pixels. All intensity profiles were background subtracted and normalized to the frame taken at the end of registration. For presentation purposes, images were exported in Artstudio Pro version 2.0.13 (Lucky Clan, Lodz, Poland; http://www.luckyclan.com) for adjustments of brightness and contrast.

Video Files

Time-lapse image sequences were converted from the czi file format to audio-video interleave (AVI) movies using Fiji software (National Institutes of Health; https://imagej.net/Fiji).

Video 1. Time-lapse video of CHO-hCB_1R cells labeled with 0.2 μM **3b** for 10 min. Time-lapse image sequences were converted from the czi file format to audio-video interleave (AVI) movies using Fiji.

Video 2. Time-lapse video of CHO-hCB_2R cells labeled with 0.2 μM **3b** for 10 min**.** Time-lapse image sequences were converted from the czi file format to audio-video interleave (AVI) movies using Fiji.

Video 3. Time-lapse video of murine splenocytes incubated with 0.05% DMSO (vehicle) for 10 min to assess video background.

Video 4. Time-lapse video of murine splenocytes labeled with 0.4 μM **3b** for 10 min.

Video 5. Time-lapse video of murine splenocytes labeled with 0.4 μM **3b** in presence of 4 μM of JWH-133 for 10 min.

Video 6. Time-lapse video of human macrophages labeled with 0.6 μM **3b** for 10 min.

Video 7. Time-lapse video of human macrophages labeled with 0.6 μM **3b** in presence of 4 μM of JWH-133 for 10 min.

Spleen cell extraction and culturing

Two-month-old male mice (C57BL6/j6) were sacrificed by decapitation according to institutional guidelines, spleen was extracted and washed in complete medium (RPMI 1640 medium without Ca^{2+} and Mg^{2+}, supplemented with 10% heat inactivated FBS (HyClone, Logan, UT, USA), 10 U/mL penicillin/streptomycin and 2 mM L-glutamine). The spleen was cut in small cubes of approximately 1 mm^3 of volume by using a sterile scalpel. Spleen samples were then placed in a 27 mm Nunc Glass Base dish (Thermo Fisher Scientific, Monza, Italy) with 5 mL of complete medium and incubated for 1 hour at 37 °C and 5% CO_2. Splenocytes were separated by passing the spleen cubes in serial pipette tips of different size. The cells were counted using a counting chamber, Imp. Neubauer, 25×75 mm (NanoEntek, Seoul, South Korea) and $5x10^5$ cells were seeded in each well of a 8-well sterile Lab-Tek chambered 1.0 borosilicate coverglass (Thermo Fisher Scientific) with 400 μL complete medium and incubated at 37°C and 5% CO_2 until imaging experiments. Mice were handled according to ethical

regulations on the use and welfare of experimental animals of the European Union (EU Directive 2010/63/EU) and the Italian Ministry of Health (art. 31, D.lgs. 26/2014), and the procedures were approved by the bioethical committee of Fondazione Santa Lucia of Rome (protocol n. 421/2019-PR).

Human primary macrophages

To obtain human macrophages, peripheral blood mononuclear cells from 40-50 years old healthy male donors were isolated by Ficoll density gradient centrifugation. CD14+ human monocytes were further isolated by leukocytes by means of immunomagnetic sorting, plated onto 24-well plates, and were differentiated into monocyte-derived macrophages in 1640 RPMI medium, containing 10% heat-inactivated fetal bovine serum, 5% heat-inactivated human serum, 100 U/mL penicillin/streptomycin and supplemented with 25 ng/ml premium grade macrophage colony-stimulating factor (Miltenyi Biotec, Bologna, Italy), and were incubated in a humidified atmosphere containing 5% CO_2 at 37°C. Cell cultures were periodically washed every 48 h in order to eliminate non adherent cells (i.e., undifferentiated monocytes). After 6-8 days, adherent cells were considered as naïve M0 (M2-like) macrophages and were used for further experiments.[15] All donors gave informed consent, and the study protocol was approved the bioethical committee of Fondazione Santa Lucia of Rome (CE/Prog. 589).

GENERAL SYNTHETIC METHODS

Unless otherwise noted, all reactions were carried out under N_2 atmosphere, and all reagents were purchased from commercial suppliers and used without further purification. Fluorescent dyes were purchased from Dyomics GmbH and ATTO-TEC GmbH. Analytical thin layer chromatography (TLC) was performed on Merck silica gel 60 F_{254} TLC glass plates and analytes were visualized by fluorescence quenching (using 254 nm light); and stained by potassium permanganate solution ($KMnO_4$ (3 g), K_2CO_3 (20 g), 5% aq. NaOH (5 mL), water (300 mL)) or "Seebach's magic stain" (Phosphomolybdic acid (2.5 g), $Ce(SO_4)_2$ (1 g), conc. H_2SO_4 (6 mL), H_2O (94 mL)) followed by heating. Purification of reaction products was carried out by flash chromatography using Sigma Aldrich silica 230-400 mesh particle size, 60 Å under 0.3-0.5 bar overpressure or by preparative HPLC (Waters Auto Purification System, Reprosil Gold 120 C18 125 x 20 mm column). NMR spectra were acquired on Bruker AVIII HD 600 MHz, 500 MHz and 400 MHz spectrometers, Bruker Neo 500 MHz and 400 MHz spectrometers, operating at the denoted spectrometer frequency given in MHz for the specified nucleus. All experiments were acquired at 298.0 K with a calibrated Bruker Variable Temperature Controller unless otherwise noted. The chemical shifts are reported in parts per million (ppm) and coupling constants (*J*) are given in Hertz (Hz). ^{1}H NMR spectra are reported with the solvent resonance as the reference unless noted otherwise ($CDCl_3$ at 7.26 ppm, CD_3OD at 3.31 ppm, CD_2Cl_2 at 5.32 ppm). Peaks are reported as (s = singlet, d = doublet, t = triplet, q = quartet, m = multiplet or unresolved, br = broad signal, coupling constant(s) in Hz, integration). ^{13}C NMR spectra were recorded with ^{1}H-decoupling and are reported with the solvent resonance as the reference unless noted otherwise ($CDCl_3$ at 77.16 ppm, CD_3OD at 49.00 ppm, CD_2Cl_2 at 54.00 ppm). Service measurements were performed by the NMR service team of the Laboratorium für Organische Chemie at ETH Zürich. Infrared (IR) spectra were measured neat on a Perkin-Elmer UATR Two Spectrometer. Band maxima are reported in wavenumbers (cm^{-1}). High-resolution mass spectrometric data were obtained at the mass spectrometry service operated by the Laboratory of Organic Chemistry at the ETHZ on VG-TRIBRID for electron impact ionization (EI), Varian IonSpec Spectrometer for electrospray ionization (ESI) or IonSpec Ultima Fourier Transform Mass Spectrometer for matrix-assisted laser desorption/ionization (MALDI), and are reported as (m/z). Optical rotations were measured with a Jasco P-2000 Polarimeter (10 cm, 1.5 mL cell).

COMPOUND SYNTHESIS AND CHARACTERIZATION

Synthesis of 2[16]

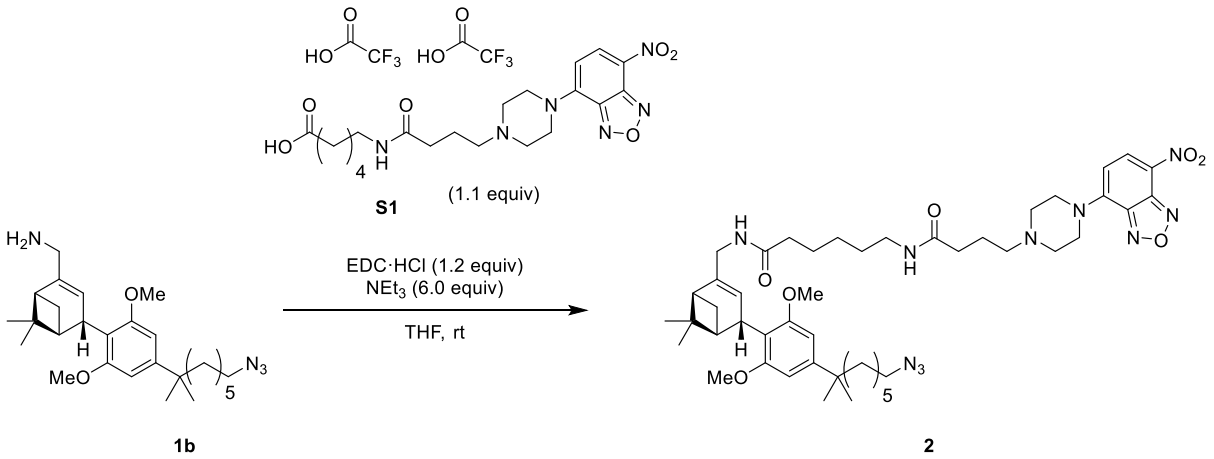

Furazane-dye **S1** (19 mg, 0.028 mmol, 1.1 equiv) was dissolved in THF (0.3 mL) and combined with NEt_3 (20 μL, 0.14 mmol, 5.4 equiv). EDC·HCl (6.2 mg, 0.032 mmol, 1.2 equiv) was added and it was stirred for 5 minutes at ambient temperature, before a solution of amine **1b** (12 mg, 0.026 mmol, 1.0 equiv) in THF (0.3 mL) was added. The mixture was concentrated under a stream of nitrogen to a volume of about 0.3 mL and stirred at ambient temperature. After 3 h, the mixture was diluted with EtOAc (100 mL), washed with water (10 mL) and brine (2 x 10 mL), dried over $MgSO_4$, filtered and concentrated. The residue was purified by preparative TLC (CH_2Cl_2:hexanes:MeOH 10:3:1) to afford the title compound as orange oil (13 mg, 0.015 mmol, 56%).

R_f = 0.37 (CH_2Cl_2:hexanes:MeOH 10:3:1; orange spot, $KMnO_4$, UV). **^{1}H NMR** (400 MHz, $CDCl_3$) δ = 8.41 (d, *J* = 8.9 Hz, 1H), 6.47 (s, 2H), 6.29 (d, *J* = 9.0 Hz, 1H), 5.86 (s, 1H), 5.60 (dt, *J* = 2.9, 1.5 Hz, 1H), 5.37 (t, *J* = 5.7 Hz, 1H), 4.11 (t, *J* = 4.9 Hz, 4H), 3.99 – 3.93 (m, 1H), 3.93 – 3.77 (m, 2H), 3.73 (s, 6H), 3.26 (app q, *J* = 6.7 Hz, 2H), 3.21 (t, *J* = 6.9 Hz, 2H), 2.70 (t, *J* = 4.9 Hz, 4H), 2.47 (t, *J* = 7.1 Hz, 2H), 2.25 (t, *J* = 7.3 Hz, 2H), 2.22 – 2.13 (m, 3H), 2.10 – 2.03 (m, 2H), 1.89 (q, *J* = 7.1 Hz, 2H), 1.67 (t, *J* = 8.4 Hz, 3H), 1.59 – 1.49 (m, 4H), 1.43 – 1.28 (m, 6H), 1.27 (s, 3H), 1.26 (d, *J* = 4.9 Hz, 6H), 1.21 (dd, *J* = 9.2, 7.3 Hz, 2H), 1.15 – 1.06 (m, 2H), 0.94 (s, 3H). **^{13}C NMR** (101 MHz, $CDCl_3$) δ = 172.7, 172.6, 158.5, 149.5, 145.3, 145.0, 144.9, 138.5, 135.3, 124.1, 123.7, 117.6, 102.8, 102.7, 57.4, 55.9, 52.7, 51.6, 49.5, 47.4, 44.6, 44.5, 44.5, 40.9, 39.3, 38.1, 37.6, 36.6, 34.3, 30.0, 29.3, 29.0, 29.0, 28.0, 26.7, 26.5, 26.4, 25.2, 24.7, 22.6, 21.2. **IR** (neat) 3301, 3094, 2931, 2861, 2095, 1644, 1609, 1543, 1294, 1247, 1121, 997, 912, 733. **ESI-HRMS** calcd for $C_{47}H_{69}N_{10}O_7$ $[M+H]^+$ 885.5345, found 885.5345.

Synthesis of 3a

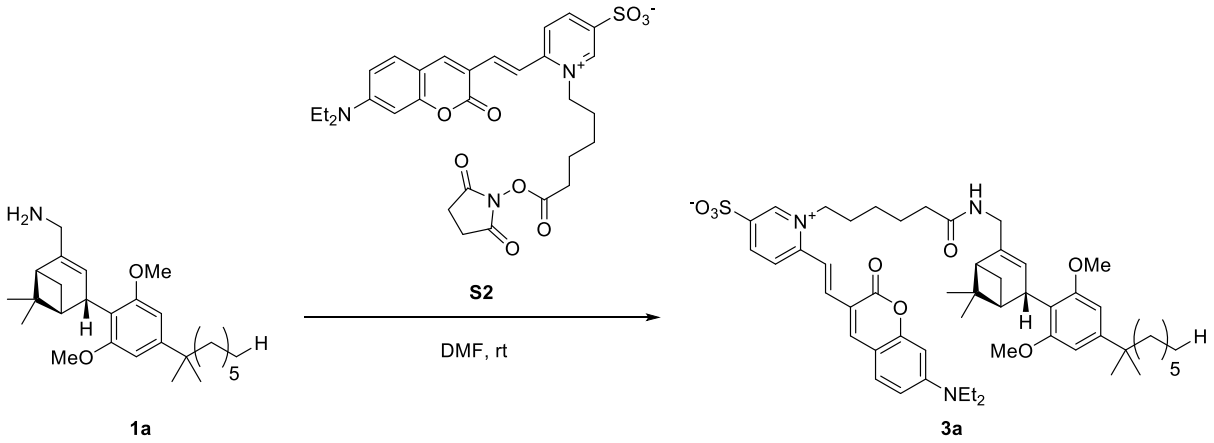

The NHS ester of DY480XL **S2** (2.0 mg, 0.0033 mmol, 1.0 equiv) was combined with a solution of amine **1a** (2.0 mg, 0.0049 mmol, 1.5 equiv) in DMF (0.13 mL) and stirred at ambient temperature until LCMS analysis indicated full consumption of the active ester (< 10 h). The product was isolated by pipette column (2% MeOH in CH_2Cl_2) as dark-red oil (2.5 mg, 0.0028 mmol, 84%).

R_f = 0.43 (10% MeOH in CH_2Cl_2; red spot, UV, Seebach). **^{1}H NMR** (500 MHz, CD_3OD) δ = 9.02 (d, *J* = 1.9 Hz, 1H), 8.58 (ddd, *J* = 8.6, 1.8, 0.6 Hz, 1H), 8.42 (d, *J* = 8.7 Hz, 1H), 8.15 (s, 1H), 8.10 (d, *J* = 15.4 Hz, 1H), 7.79 (d, *J* = 15.4 Hz, 1H), 7.52 (d, *J* = 9.1 Hz, 1H), 6.83 (dd, *J* = 9.0, 2.5 Hz, 1H), 6.56 (dd, *J* = 2.4, 0.6 Hz, 1H), 6.48 (s, 2H), 5.60 – 5.56 (m, 1H), 4.71 – 4.60 (m, 2H), 3.93 (t, *J* = 2.4 Hz, 1H), 3.86 – 3.80 (m, 1H), 3.73 – 3.71 (m, 1H), 3.69 (s, 6H), 3.56 – 3.48 (m, 4H), 2.34 – 2.27 (m, 2H), 2.16 – 2.12 (m, 1H), 2.09 – 2.00 (m, 3H), 1.97 – 1.93 (m, 1H), 1.81 – 1.74 (m, 2H), 1.72 (d, *J* = 8.4 Hz, 1H), 1.57 (dd, *J* = 7.7, 4.7 Hz, 4H), 1.25 – 1.19 (m, 21H), 1.06 (m, 2H), 0.92 (s, 3H), 0.86 – 0.83 (m, 3H). **^{13}C NMR** (126 MHz, CD_3OD) δ = 175.4, 162.1, 159.8, 158.4, 155.3, 154.5, 150.5, 149.4, 143.9, 143.5, 142.7, 142.0, 139.7, 132.3, 126.0, 123.9, 118.6, 116.7, 114.6, 111.8, 110.5, 103.8, 97.6, 56.2, 48.5, 46.1, 45.5, 45.4, 44.9, 41.8, 39.0, 38.7, 36.7, 32.9, 31.1, 30.8, 30.4, 29.6, 29.5, 28.4, 26.8, 26.8, 26.3, 25.8, 23.7, 21.4, 14.4, 12.8.**IR** 2928, 2859, 1713, 1618, 1579, 1504, 1453, 1417, 1355, 1278, 1238, 1133, 1042, 671. **ESI-HRMS** calcd for $C_{53}H_{72}N_3NaO_8S$ $[M+H]^+$ 910.5035, found 910.5008.

Synthesis of 3b

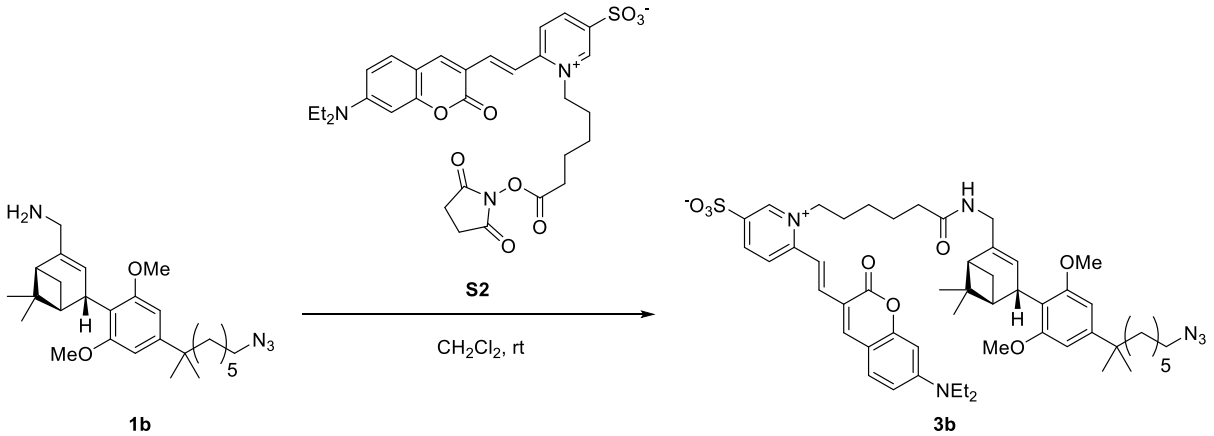

The NHS ester of DY480XL **S2** (5.0 mg, 0.0082 mmol, 1.0 equiv) was combined with a solution of amine **1b** (5.0 mg, 0.011 mmol, 1.3 equiv) in CH_2Cl_2 (0.3 mL) and stirred at ambient temperature until LCMS analysis indicated full consumption of the active ester (< 2 h). The product was isolated by preparative TLC (10% MeOH in CH_2Cl_2) as dark-red oil (7.0 mg, 0.0074 mmol, 90%).

R_f = 0.26 (10% MeOH in CH_2Cl_2; red spot, UV, Seebach). **^{1}H NMR** (500 MHz, CD_2Cl_2) δ = 9.02 (d, *J* = 1.6 Hz, 1H), 8.68 (d, *J* = 8.4 Hz, 1H), 8.18 – 8.12 (m, 2H), 7.95 (s, 1H), 7.52 (d, *J* = 15.3 Hz, 1H), 7.47 (d, *J* = 9.0 Hz, 1H), 6.73 (dd, *J* = 9.0, 2.5 Hz, 1H), 6.54 (d, *J* = 2.4 Hz, 1H), 6.51 (s, 1H), 6.00 (t, *J* = 5.8 Hz, 1H), 5.63 (dt, *J* = 2.9, 1.5 Hz, 1H), 4.61 (t, *J* = 8.2 Hz, 2H), 3.99 – 3.96 (m, 1H), 3.92 – 3.82 (m, 2H), 3.75 (d, *J* = 6.3 Hz, 6H), 3.50 (q, *J* = 7.2 Hz, 4H), 3.25 (t, *J* = 7.0 Hz, 2H), 2.29 (t, *J* = 7.5 Hz, 2H), 2.21 – 2.16 (m, 1H), 2.16 – 2.12 (m, 1H), 2.12 – 2.06 (m, 2H), 2.03 (tt, *J* = 5.9, 1.9 Hz, 1H), 1.78 (q, *J* = 7.5 Hz, 2H), 1.72 (d, *J* = 8.3 Hz, 1H), 1.65 – 1.53 (m, 6H), 1.37 – 1.32 (m, 2H), 1.31 – 1.24 (m, 17H), 1.15 (qd, *J* = 8.1, 4.8 Hz, 2H), 0.98 (s, 3H). **^{13}C NMR** (126 MHz, CD_2Cl_2) δ = 172.3, 160.6, 158.9, 157.4, 153.4, 153.0, 149.8, 147.8, 145.5, 142.8, 142.3, 141.2, 139.1, 131.2, 124.7, 123.6, 117.9, 115.8, 113.7, 110.7, 109.3, 103.1, 97.1, 59.2, 56.1, 56.1, 51.9, 47.9, 45.6, 44.7, 44.6, 44.6, 41.1, 38.3, 37.9, 36.3, 30.2, 29.8, 29.2, 29.1, 27.9, 27.0, 26.5, 26.2, 25.0, 25.0, 21.2, 12.6. **IR** 3332, 3059, 2932, 2863, 2096, 1713, 1618, 1580, 1505, 1417, 1355, 1272, 1238, 1134, 1042, 671. **ESI-HRMS** calcd for $C_{53}H_{70}N_6NaO_8S$ $[M+Na]^+$ 973.4868, found 973.4857.

Synthesis of S3

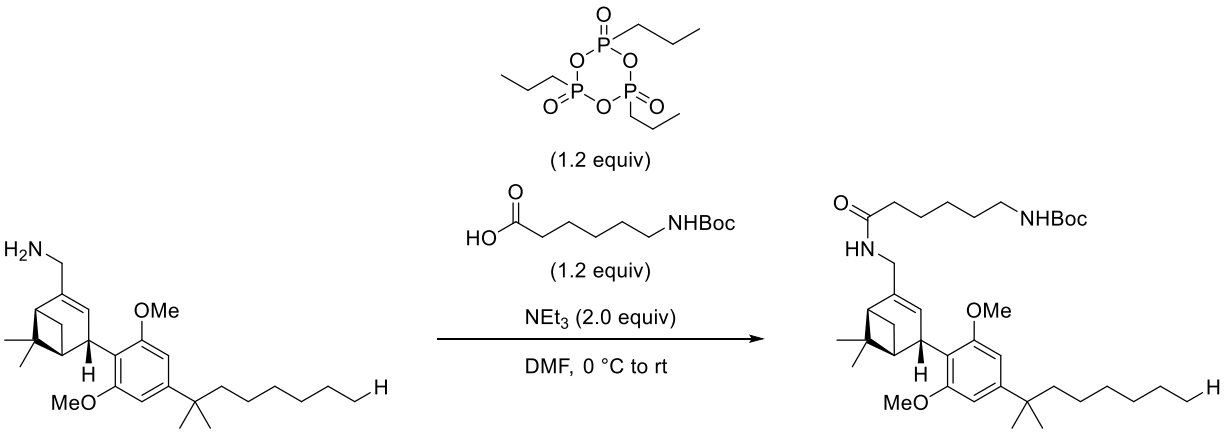

To a solution of 6-(Boc-amino)hexanoic acid (33.5 mg, 0.145 mmol, 1.20 equiv) and **1a** (50 mg, 0.12 mmol, 1.0 equiv) in DMF (0.6 mL) at 0 °C was added propylphosphonic anhydride (50 wt% in DMF, 0.85 μL, 0.15 mmol, 1.2 equiv) and NEt_3 (34 μL, 0.24 mmol, 2.0 equiv). The resulting yellow solution was allowed to warm to ambient temperature and was stirred for 20 h. The reaction was then stopped by addition of water. After dilution with EtOAc (20 mL) and separation of the organic phase, the aqueous layer was extracted with EtOAc (3 x 10 mL). The combined organic layers were washed with water, sat. aq. $NaHCO_3$, 5 wt% aq. LiCl and brine, dried over Na_2SO_4 and concentrated under reduced pressure. Purification by flash chromatography (hexanes/EtOAc 9:1, then 1:1) afforded the product as yellow oil (45 mg, 0.0072 mmol, 59% yield).

^{1}H NMR (400 MHz, $CDCl_3$) δ = 6.48 (s, 2H), 5.62 – 5.59 (m, 1H), 5.33 (s, 1H), 4.52 (s, 1H), 3.96 (t, *J* = 2.3 Hz, 1H), 3.92 – 3.79 (m, 2H), 3.73 (s, 6H), 3.14 – 3.07 (m, 2H), 2.23 – 2.14 (m, 3H), 2.11 – 2.04 (m, 2H), 1.72 – 1.62 (m, 3H), 1.58 – 1.53 (m, 2H), 1.52 – 1.46 (m, 2H), 1.43 (s, 9H), 1.40 – 1.33 (m, 2H), 1.28 (s, 3H), 1.26 (s, 6H), 1.24 – 1.19 (m, 6H), 1.14 – 1.06 (m, 2H), 0.95 (s, 3H), 0.87 – 0.83 (m, 3H).**^{13}C NMR** (101 MHz, $CDCl_3$) δ = 172.7, 158.5, 156.1, 149.7, 138.5, 124.0, 117.5, 102.9, 79.2, 56.0, 47.4, 44.7, 44.6, 44.5, 40.9, 40.5, 38.1, 37.6, 37.0, 32.0, 30.2, 30.0, 29.1, 28.6, 28.0, 26.6, 26.4, 25.6, 24.8, 22.8, 21.2, 14.2 **IR** 3320, 2929, 2861, 1695, 1648, 1606, 1572, 1533, 1453, 1411, 1365, 1238, 1173, 1123. **ESI-HRMS** calcd for $C_{38}H_{63}N_2O_5$ $[M+H]^+$ 627.4731; found 627.4723. $\mathbf{[\alpha]_D^{25}}$ = +62.4 (c = 1.0, $CHCl_3$).

Synthesis of 4

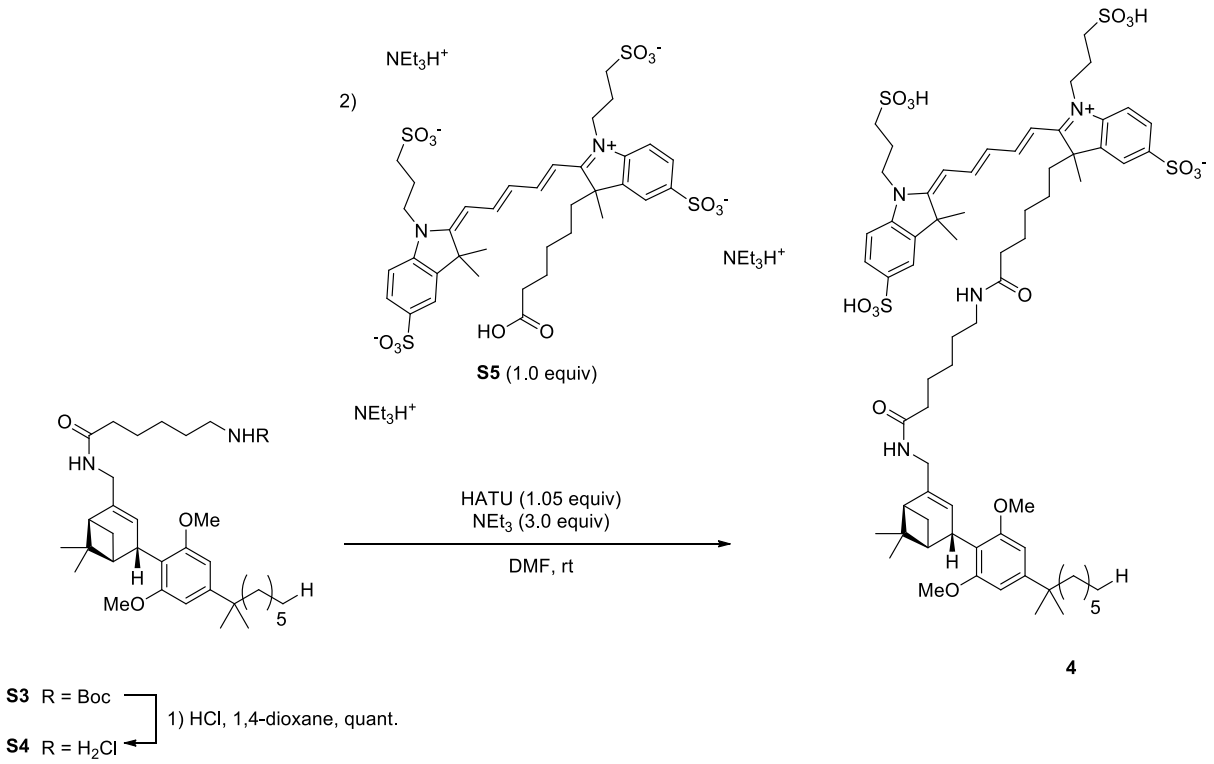

To a solution of **S3** (4.3 mg, 0.0064 mmol, 1.5 equiv) in dioxane (0.032 mL) was added 4.0 M HCl in dioxane (0.0081 mL, 0.032 mmol, 7.5 equiv) and it was stirred for 1 hour at ambient temperature. The solvent was removed under a stream of nitrogen followed by high vacuum. The obtained hydrochloride was used as is in the subsequent step.

The (tris)triethylammonium salt **S5** of Alexa647 carboxylic acid (5.0 mg, 0.0043 mmol, 1.0 equiv) was combined with a solution of hydrochloride **S4** (3.6 mg, 0.0064 mmol, 1.5 equiv) in DMF (0.043 mL). Then, NEt_3 (1.8 μL, 0.013 mmol, 3.0 equiv) and HATU (1.7 mg, 0.0045 mmol, 1.0 equiv) were added to the reaction mixture and it was left to stir for 15 h. Since conversion was observed to be incomplete, HATU (0.8 mg, 0.002 mmol, 0.5 equiv) was re-added to the reaction mixture and the mixture was left to stir for another 2 hours upon which full conversion was monitored by TLC. The mixture was diluted with H_2O and MeOH and lyophilized to remove the solvent. The crude product was further purified by flash chromatography (superneutral silica, dry loading, 20% MeOH in CH_2Cl_2 to 10% water/20% isopropyl alcohol in ethyl acetate to 20% water/40% isopropyl alcohol in ethyl acetate) to remove co-eluting HOAt contaminant. Further purification by preparative TLC (20% water/40% isopropyl alcohol in ethyl acetate) furnished the product (1.8 mg, 0.0011 mmol, 26%) as deep blue oil.

$\mathbf{R_f}$ = 0.42 (20% water/40% isopropyl alcohol in ethyl acetate; blue spot, UV). **^{1}H NMR** (600 MHz, CD_3OD) δ = 8.35 (q, *J* = 12.5 Hz, 2H), 7.92 – 7.89 (m, 3H), 7.86 (d, *J* = 1.7 Hz, 1H), 7.46

(d, *J* = 8.6 Hz, 1H), 7.43 (dd, *J* = 8.4, 2.9 Hz, 1H), 6.75 (t, *J* = 12.4 Hz, 1H), 6.53 – 6.46 (m, 2H), 6.51 (s, 2H), 5.57 – 5.55 (m, 1H), 4.38 – 4.33 (m, 4H), 3.97 – 3.95 (m, 1H), 3.79 (dt, *J* = 15.2, 1.8 Hz, 1H), 3.72 (dt, *J* = 15.2, 1.8 Hz, 1H), 3.71 (d, *J* = 1.0 Hz, 6H), 3.06 (tt, *J* = 7.1, 1.7 Hz, 2H), 2.98 (q, *J* = 6.8 Hz, 4H), 2.46 (t, *J* = 13 Hz, 1H), 2.28 – 2.19 (m, 7H), 2.15 – 2.13 (m, 1H), 2.08 (td, *J* = 5.7, 1.4 Hz, 1H), 2.00 – 1.96 (m, 3H), 1.77 – 1.72 (m, 10H), 1.62 – 1.58 (m, 4H), 1.47 – 1.43 (m, 4H), 1.33 – 1.31 (m, 2H), 1.27 (s, 3H), 1.26 (s, 6H), 1.24 – 1.19 (m, 8H), 1.10 – 1.05 (m, 2H), 0.95 – 0.93 (m, 1H), 0.94 (s, 3H), 0.85 (t, *J* = 6.9 Hz, 3H), 0.66 – 0.57 (m, 1H). **^{13}C NMR** (151 MHz, CD_3OD) δ = 175.9, 175.8, 175.5, 173.7, 159.8, 159.8, 156.8, 156.0, 150.4, 145.8, 144.9, 143.5, 143.4, 142.6, 140.8, 139.8, 128.5, 128.2, 128.1, 124.0, 121.4, 121.3, 118.7, 111.8, 111.5, 105.8, 105.6, 103.8, 103.8, 56.2, 56.2, 55.1, 50.7, 48.9, 49.3, 49.3, 45.5, 45.5, 44.9, 44.2, 44.1, 42.1, 41.8, 40.2, 39.0, 38.7, 37.1, 36.6, 32.9, 31.1, 30.0, 29.9, 29.6, 29.6, 28.4, 27.8, 27.8, 27.8, 27.6, 26.9, 26.9, 26.3, 25.8, 25.1, 24.3, 24.1, 23.7, 21.4, 14.4. **IR** 2368, 2929, 1571, 1489, 1445, 1385, 1190, 1153, 1116, 1024, 980, 689, 616. **ESI-HRMS** calcd for $C_{69}H_{99}N_4O_{16}S_4$ $[M]^+$ 1367.5933; found 1367.5948**.**

Synthesis of S6

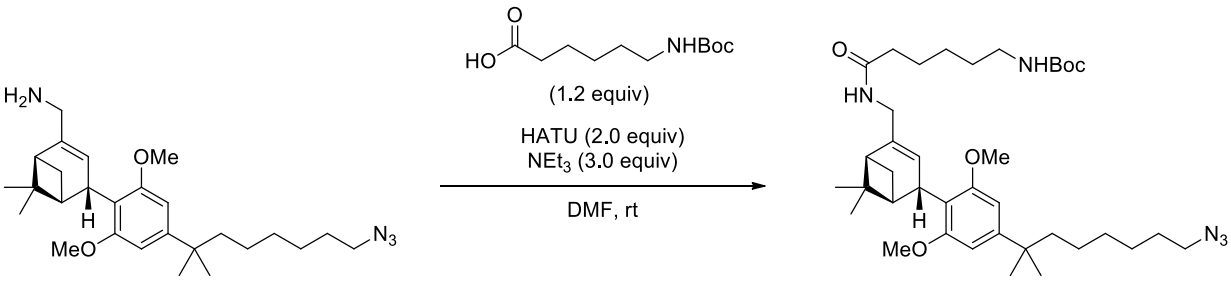

1b **S6**

To a solution of **1b** (0.008 g, 0.02 mmol, 1.0 equiv) and 6-((*tert*-butoxycarbonyl)amino)hexanoic acid (0.006 g, 0.03 mmol, 1.5 equiv) in anhydrous DMF (0.18 mL) at 0 °C was added HATU (0.01 g, 0.04 mmol, 2.0 equiv) and NEt_3 (0.007 mL, 0.05 mmol, 3.0 equiv) and the resulting yellow solution was stirred at ambient temperature for 18 h. The reaction was stopped by addition of water (1 mL) and the aqueous layer was extracted with Et_2O (3x5 mL). The combined organic extracts were washed with water and brine, dried over Na_2SO_4 and concentrated under reduced pressure. Purification of the crude material by flash column chromatography (SiO_2; using 30 to 70% EtOAc in hexanes), followed by further purification by preparative TLC (5% MeOH in CH_2Cl_2) afforded the product as faintly yellow oil (10 mg, 85% yield).

^{1}H NMR (500 MHz, $CDCl_3$) δ = 6.47 (s, 2H), 5.62 – 5.59 (m, 1H), 5.37 – 5.31 (m, 1H), 4.53 (s, 1H), 3.96 (t, *J* = 2.3 Hz, 1H), 3.91 – 3.79 (m, 2H), 3.73 (s, 6H), 3.22 (t, *J* = 6.9 Hz, 2H), 3.10 (q, *J* = 6.8 Hz, 2H), 2.22 – 2.14 (m, 3H), 2.11 – 2.03 (m, 2H), 1.72 – 1.62 (m, 3H), 1.59 – 1.47 (m, 9H), 1.43 (s, 6H), 1.39 – 1.29 (m, 4H), 1.28 (s, 6H), 1.27 (s, 3H), 1.25 – 1.19 (m, 2H), 1.16 – 1.07 (m, 2H), 0.95 (s, 3H). **^{13}C NMR** (126 MHz, $CDCl_3$) δ = 172.7, 158.5, 156.1, 149.4, 138.6, 124.0, 117.6, 102.8, 79.2, 55.9, 51.6, 47.4, 44.6, 44.6, 44.5, 40.9, 40.5, 38.1, 37.6, 36.9, 30.0, 29.8, 29.0, 29.0, 28.6, 28.0, 26.7, 26.6, 26.4, 25.6, 24.7, 21.2. **IR** (neat, ν_{max}/cm^{-1}) 3328, 2925, 2855, 2096, 1701, 1650, 1519, 1461, 1365, 1239, 1123. **ESI-HRMS** calcd for $C_{38}H_{61}N_5NaO_5$ 690.4565 $[M+Na]^+$; found 690.4556

Synthesis of 5

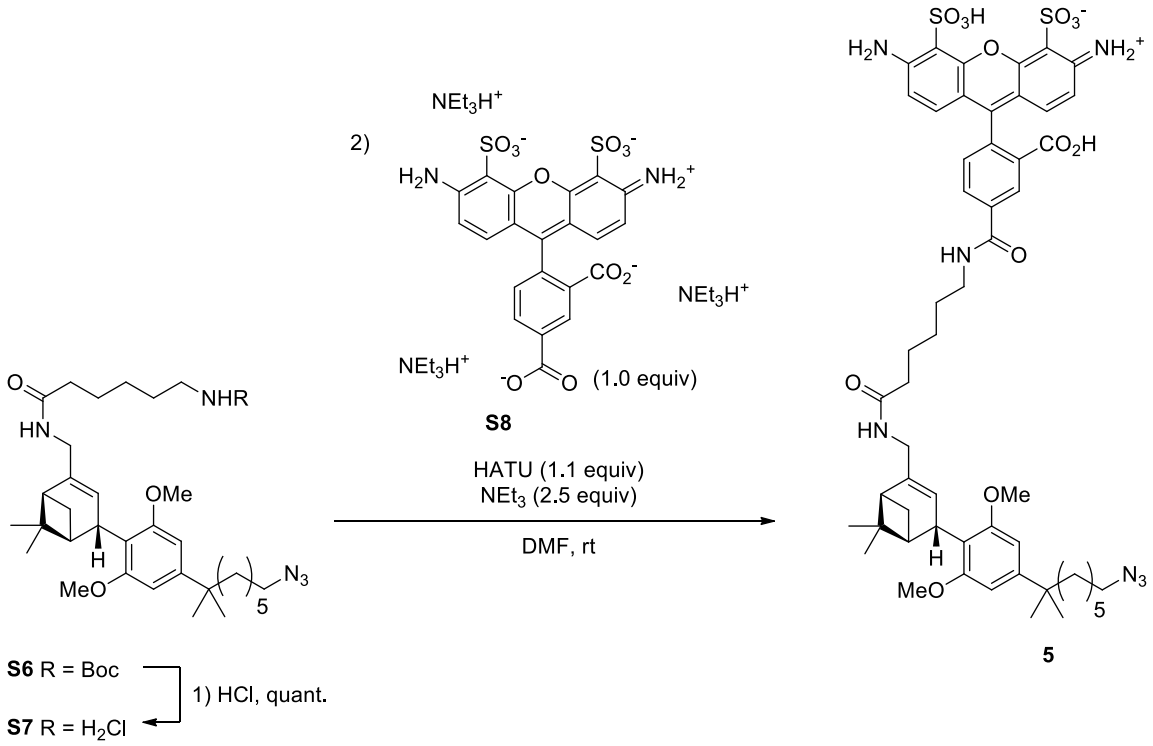

To a solution of **S6** (9.0 mg, 0.013 mmol, 2.0 equiv) in dioxane (0.14 mL) was added 2.0 M HCl in ether (0.051 mL, 0.10 mmol, 17 equiv) and the mixture was stirred for 1 hour at ambient temperature. The solvent was removed under a stream of nitrogen followed by high vacuum. The obtained hydrochloride was used without further purification in the subsequent step.

A solution of hydrochloride **S7** (8.0 mg, 0.013 mmol, 2.2 equiv) in DMF (0.1 mL) was added to the **S8** (5.0 mg, 6.0 μmol, 1.0 equiv) NEt_3 (4.2 μL, 0.030 mmol, 5.0 equiv) and HATU (2.5 mg, 6.6 μmol, 1.1 equiv) were added. The reaction mixture was stirred at ambient temperature overnight. Another portion of HATU (1.1 mg, 3.0 μmol, 0.5 equiv) was added and stirring was continued for 20 hours. Water was added and all volatiles were removed by lyophilization. Purification by preparative TLC (20% water 40% ^{i}PrOH 40% EtOAc) did not afford pure material. Further purification by preparative reverse-phase HPLC (Reprosil Gold 120 C18 125 x 20 mm column, flow 26.5 mL/min) afforded the product as dark red solid (2 mg, 30% yield).

ESI-HRMS calcd for $C_{54}H_{63}N_7O_{13}S_2$ 540.6968 $[M-H]^{2-}$; found 540.6982. **Preparative HPLC** (Reprosil Gold 120 C18 125 x 20 mm column, flow 26.5 mL/min) H_2O (+ 0.1% HCOOH):MeCN (+ 0.1% HCOOH) = 30:70 (t = 0.0 min) → 10:90 (t = 8.0 min) → 10:90 (t = 9.0 min) → 10:90 (t

= 12.0 min), t_R = 4.55 min. **Analytical HPLC** (Dr. Maisch Reprosphere C12, 5 μm, 125 x 4.6 mm, , flow 1.0 mL/min): H_2O (+ 0.1% HCOOH):MeCN (+ 0.1% HCOOH) = 40:60 (t = 0.0 min) → 10:90 (t = 10.0 min), t_R = 4.62 min.

SAMPLE INFORMATION

Sample Name:	RS-D-003	Acquired By:	EMCGroup
Sample Type:	Unknown	Sample Set Name:	RS_D003prepwithcontrol
Vial:	3	Acq. Method Set:	40_10_10min_total15min_MS
Injection #:	1	Processing Method	RSD003_prep_C12_40_2
Injection Volume:	10.00 ul	Channel Name:	500.0nm
Run Time:	15.0 Minutes	Proc. Chnl. Descr.:	PDA 500.0 nm
Date Acquired:	11/5/2019 4:16:22 PM CET		
Date Processed:	11/5/2019 4:36:51 PM CET		

Auto-Scaled Chromatogram

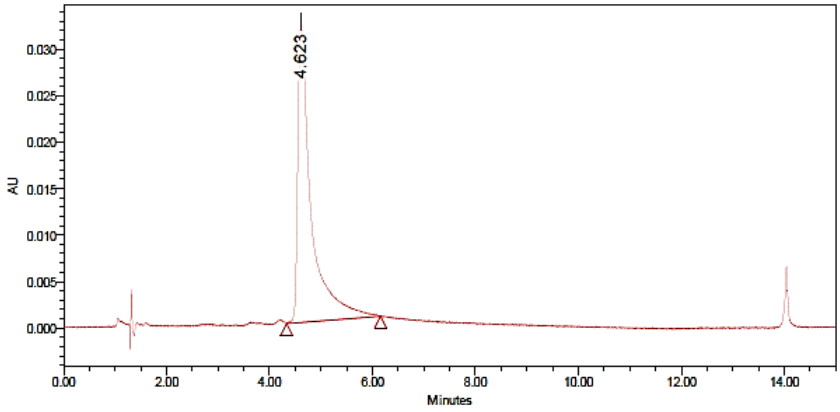

Peak Results

	Name	RT	Area	Height	Amount	Units
1		4.623	583202	32388		

PDA Result Table

	Name	RT	Purity1 Angle	Purity1 Threshold	Match1 Spect. Name	Match1 Angle	Match1 Threshold
1		4.623					

Match Plot

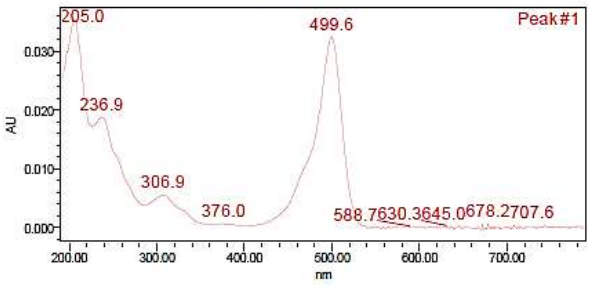

Synthesis of 6

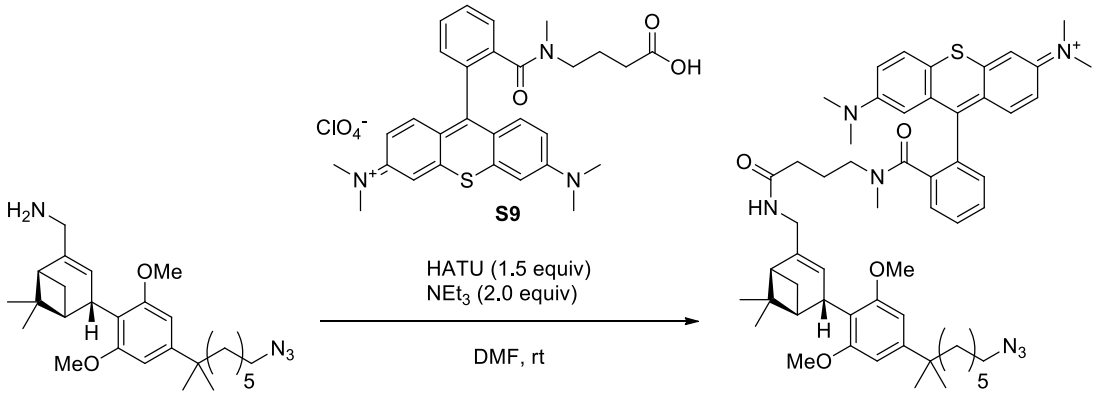

ATTO Thio12 carboxy **S9** (5.0 mg, 0.0083 mmol, 1.0 equiv) was combined with a solution of amine **1b** (5.7 mg, 0.012 mmol, 1.5 equiv) in DMF (0.17 mL). NEt_3 (2.3 mL, 0.017 mmol, 2.0 equiv) and HATU (4.7 mg, 0.012 mmol, 1.5 equiv) were added and the purple solution was stirred at ambient temperature under exclusion of light until LCMS analysis indicated full conversion of the dye (<10 h). After concentration by lyophilization the crude, purification by flash chromatography (superneutral silica, 2-3% MeOH in DCM) afforded the product as deep purple oil (6.0 mg, 0.0064 mmol, 70%).

R_f = 0.53 (10% MeOH in CH_2Cl_2; purple spot, UV, Seebach). **^{1}H NMR** (500 MHz, MeOD) δ = 7.77 – 7.72 (m, 2H), 7.68 –ff 7.63 (m, 1H), 7.50 – 7.45 (m, 1H), 7.39 (dd, *J* = 9.7, 1.0 Hz, 2H), 7.20 (dd, *J* = 15.1, 2.6 Hz, 2H), 7.11 – 7.07 (m, 2H), 6.56 (s, 2H), 5.51 (m, 1H), 4.02 – 3.95 (m, 1H), 3.80 – 3.74 (m, 1H), 3.73 (s, 6H), 3.66 – 3.60 (m, 1H), 3.29 – 3.26 (m, 12H), 3.23 – 3.16 (m, 4H), 2.87 (s, 3H), 2.13 – 2.09 (m, 1H), 2.05 – 1.97 (m, 2H), 1.70 (d, *J* = 8.4 Hz, 1H), 1.68 – 1.59 (m, 4H), 1.48 (q, *J* = 7.1 Hz, 2H), 1.42 – 1.35 (m, 2H), 1.30 – 1.26 (m, 13H), 1.15 – 1.07 (m, 2H), 0.92 (s, 3H). **^{13}C NMR** (126 MHz, MeOD) δ = 174.7, 170.6, 159.9, 159.2, 155.2, 155.2, 150.5, 145.4, 145.4, 139.8, 137.7, 137.4, 135.4, 131.6, 130.7, 130.7, 128.4, 123.6, 120.3, 120.3, 118.7, 116.5, 116.4, 106.6, 103.9, 103.8, 56.3, 52.4, 47.3, 45.5, 45.4, 44.9, 41.9, 40.8, 39.1, 38.7, 37.8, 33.9, 33.1, 30.8, 30.5, 29.8, 29.6, 29.5, 28.4, 27.6, 26.8, 25.8, 23.9, 23.7, 21.4. **IR** 2931, 2862, 2094, 1620, 1593, 1498, 1449, 1391, 1363, 1343, 1251, 1179, 1157, 1122, 842. **ESI-HRMS** calcd for $C_{56}H_{72}N_7O_4S$ $[M]^+$ 938.5361, found 938.5357.

NMR SPECTRA

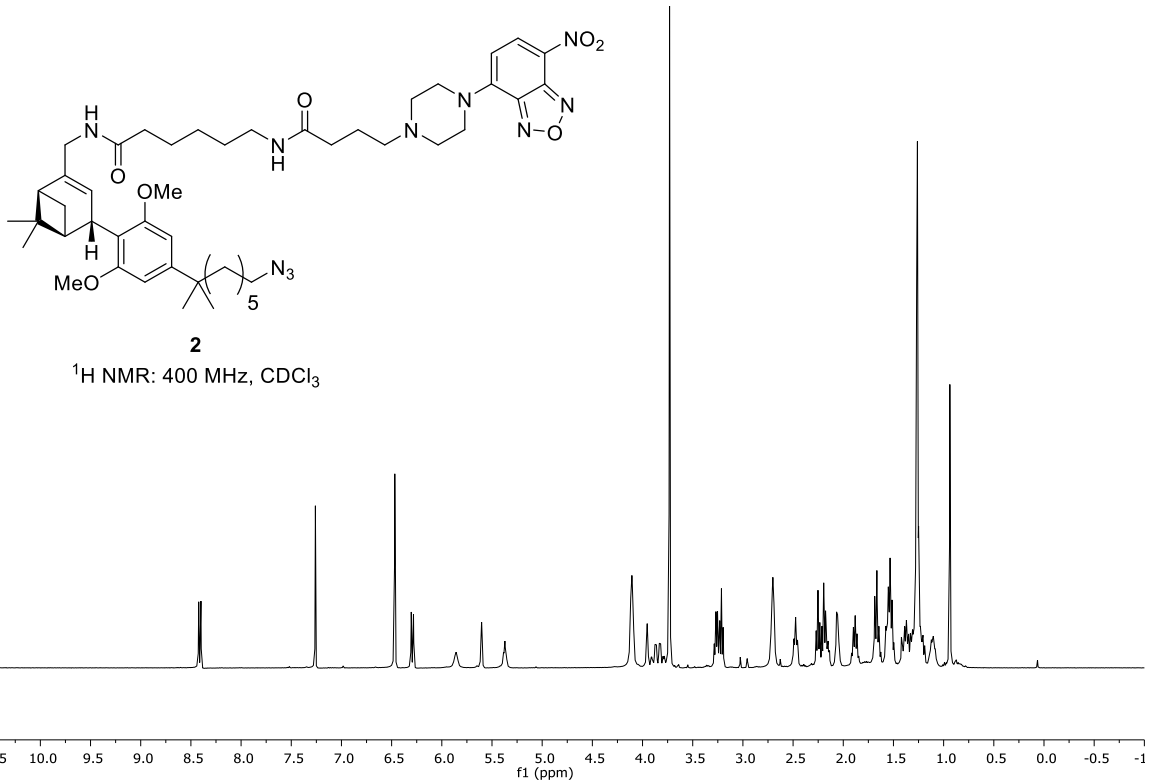

2

^{1}H NMR: 400 MHz, $CDCl_3$

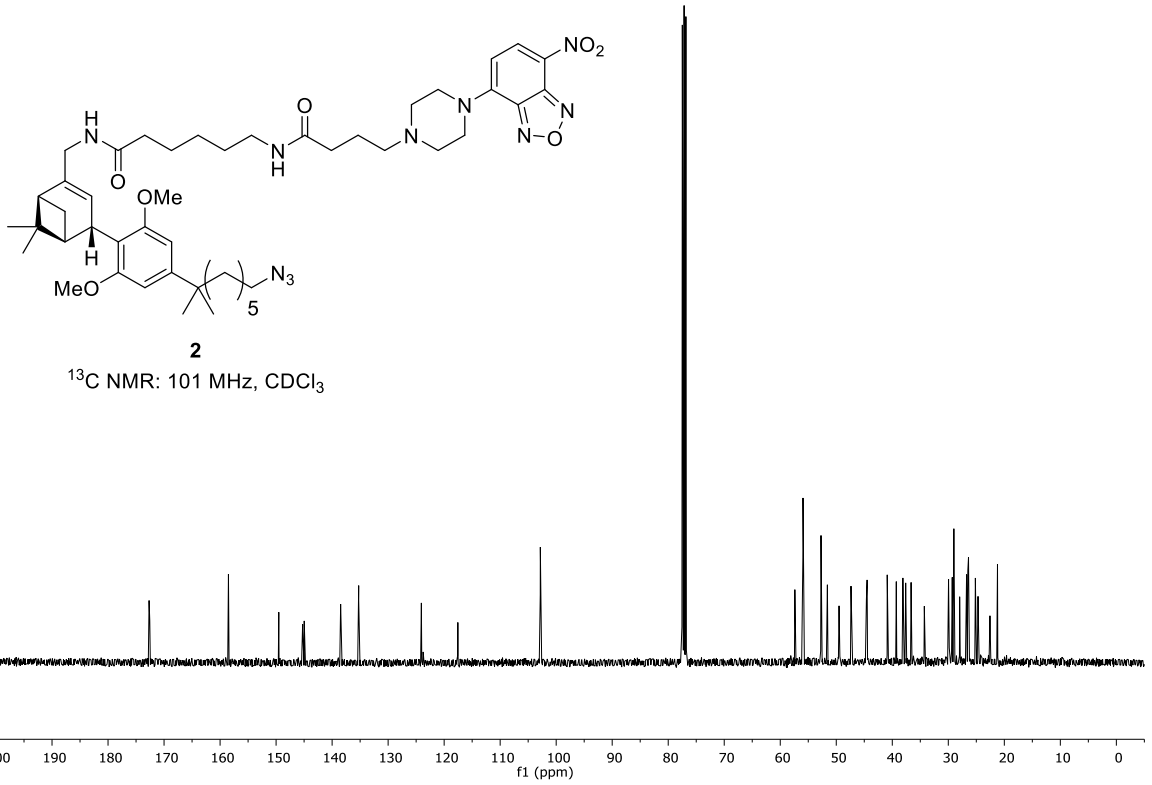

2

^{13}C NMR: 101 MHz, $CDCl_3$

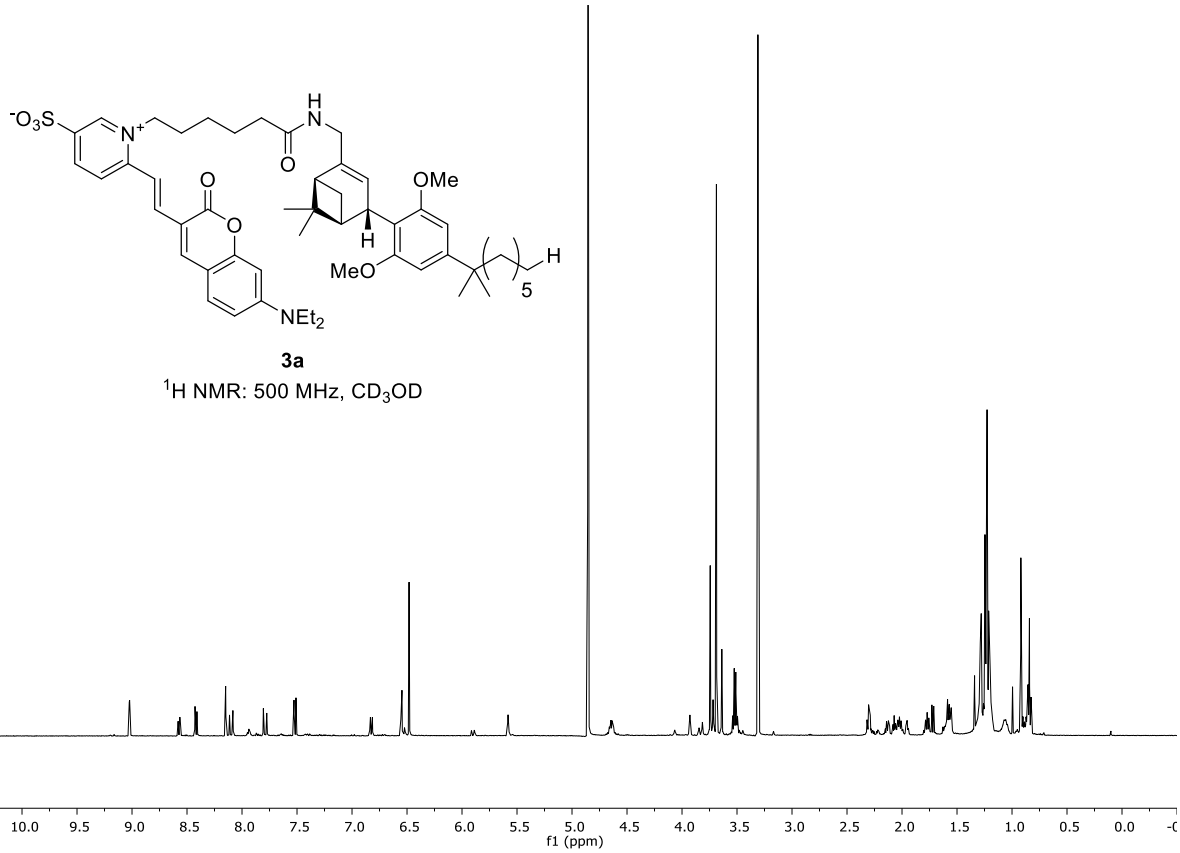

3a

^{1}H NMR: 500 MHz, CD_3OD

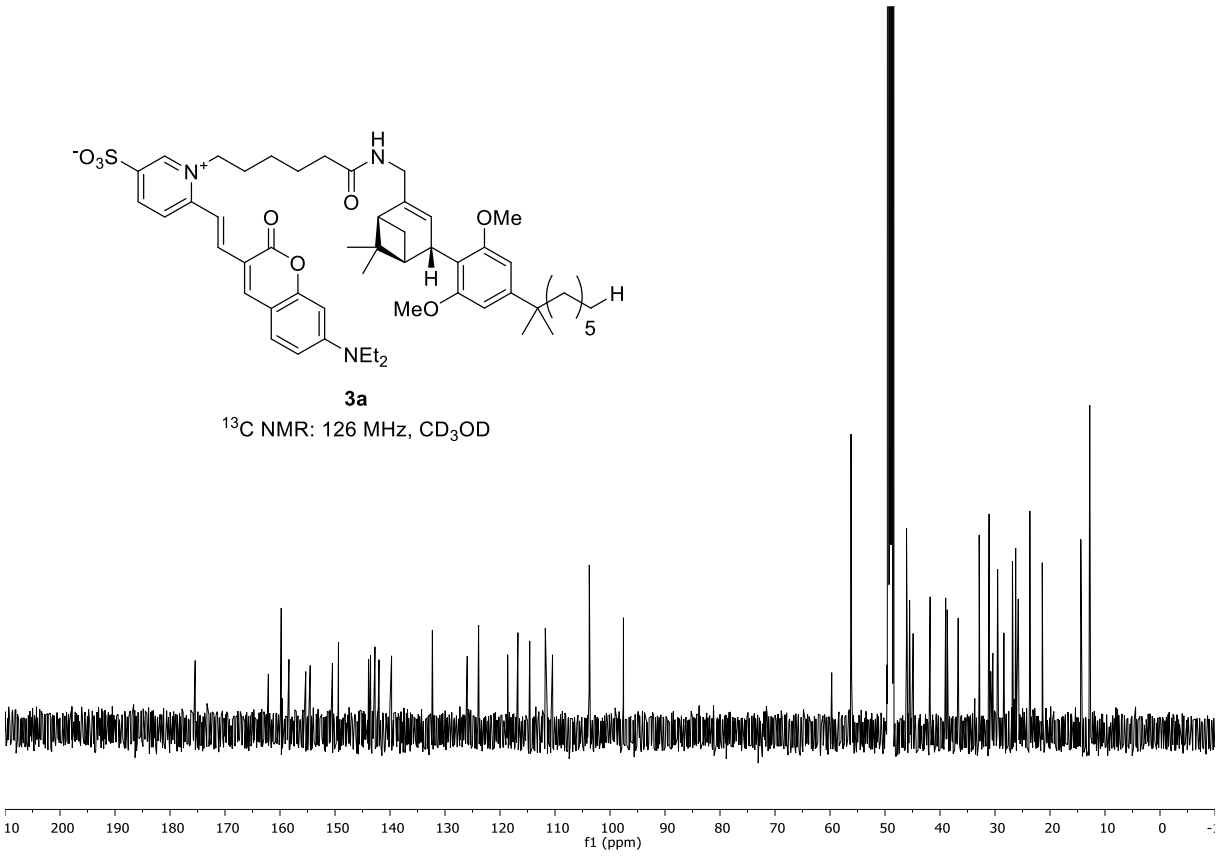

3a

^{13}C NMR: 126 MHz, CD_3OD

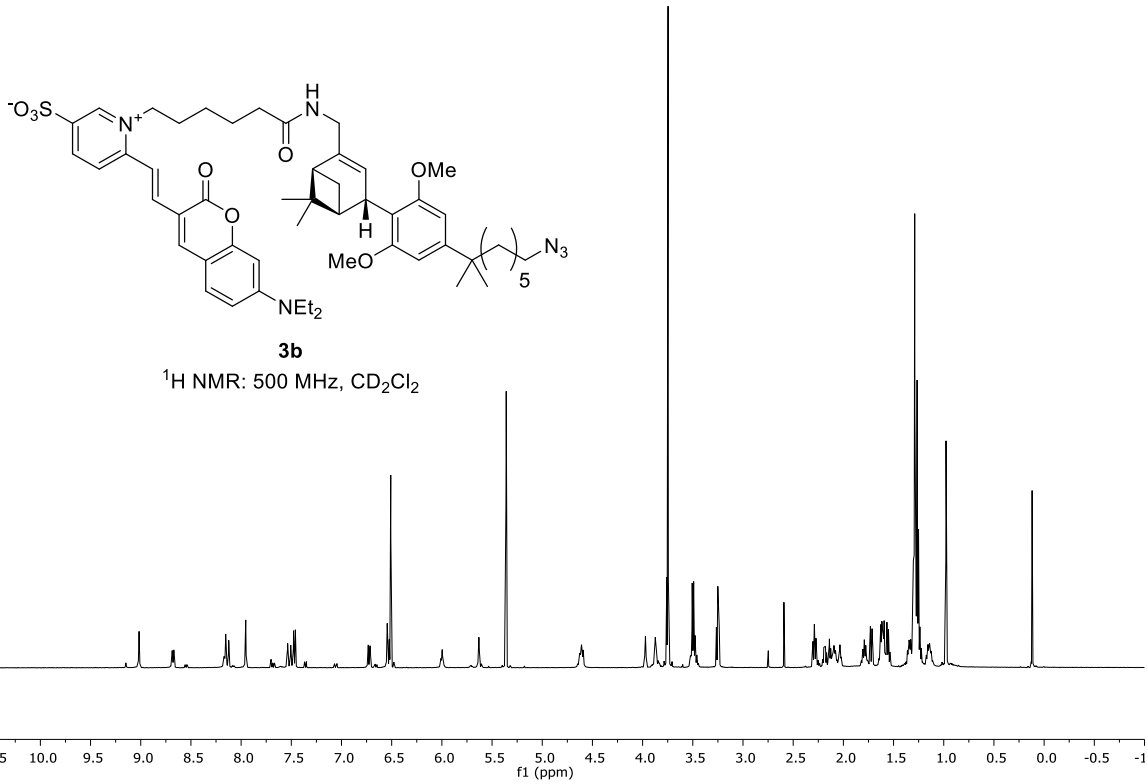

3b

^{1}H NMR: 500 MHz, CD_2Cl_2

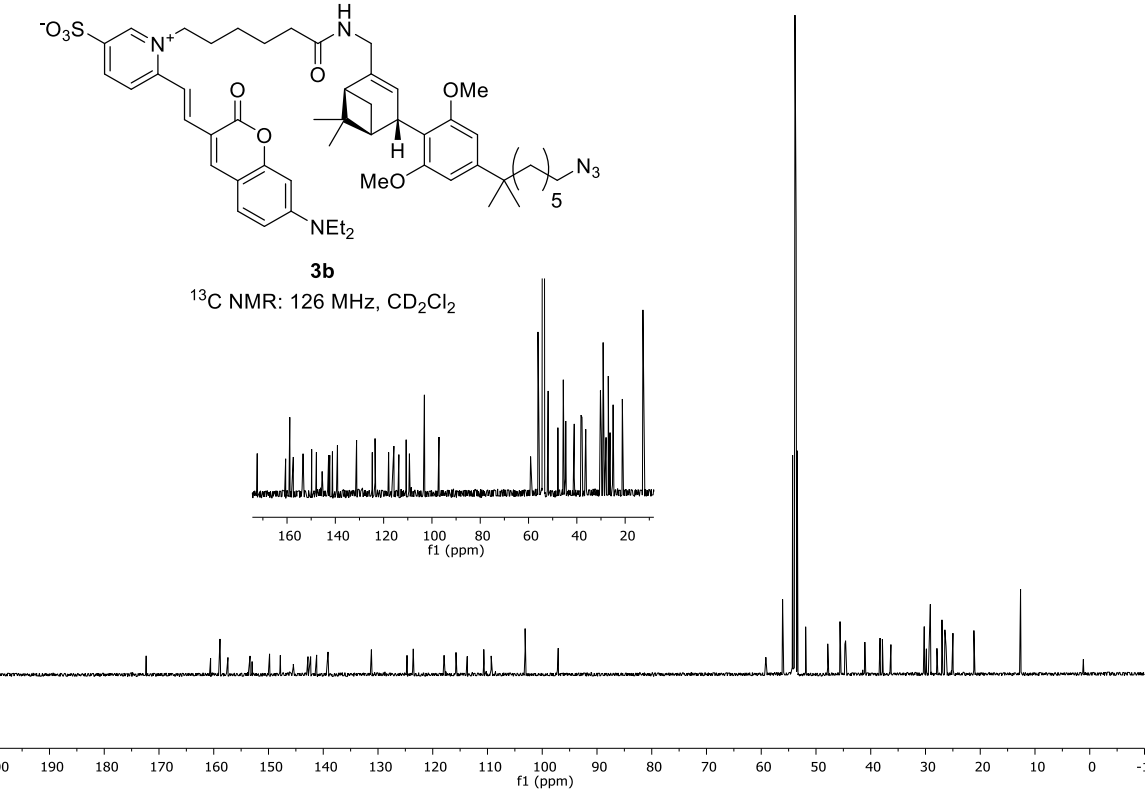

3b

^{13}C NMR: 126 MHz, CD_2Cl_2

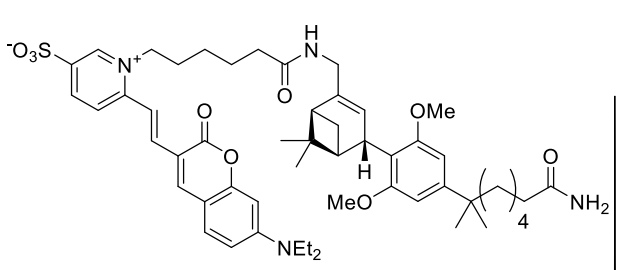

3c

^{1}H NMR: 400 MHz, CD_2Cl_2

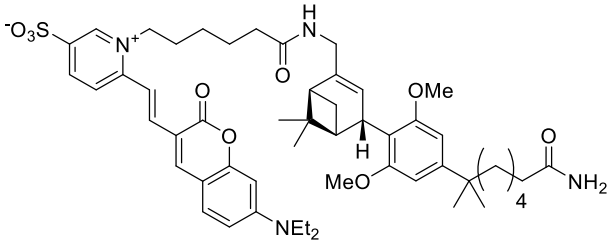

3c

^{13}C NMR: 101 MHz, CD_2Cl_2

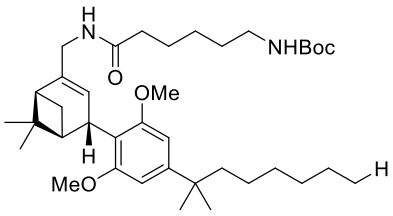

S3

^{1}H NMR: 400 MHz, $CDCl_3$

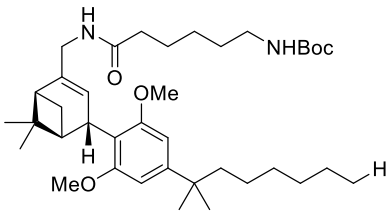

S3

^{13}C NMR: 101 MHz, $CDCl_3$

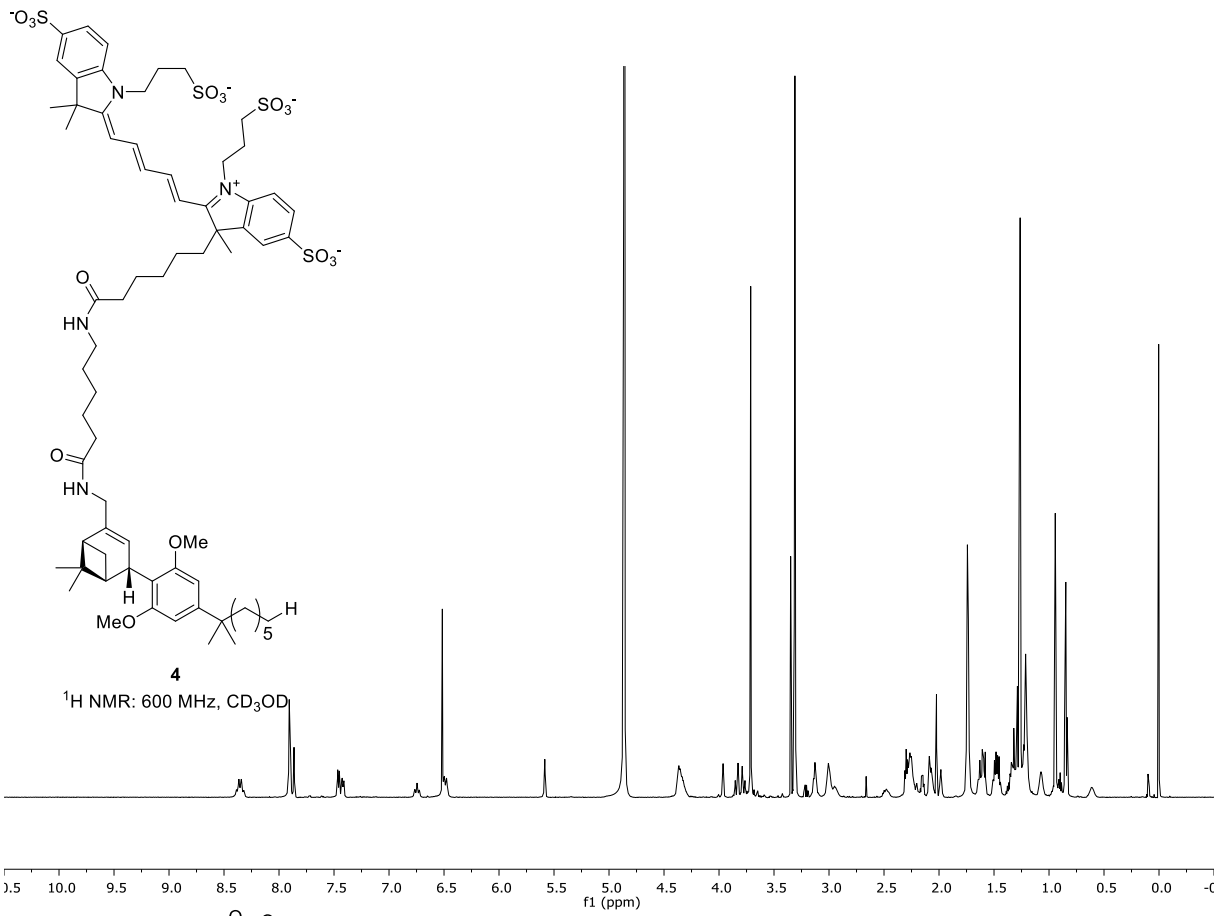

4

^{1}H NMR: 600 MHz, CD_3OD

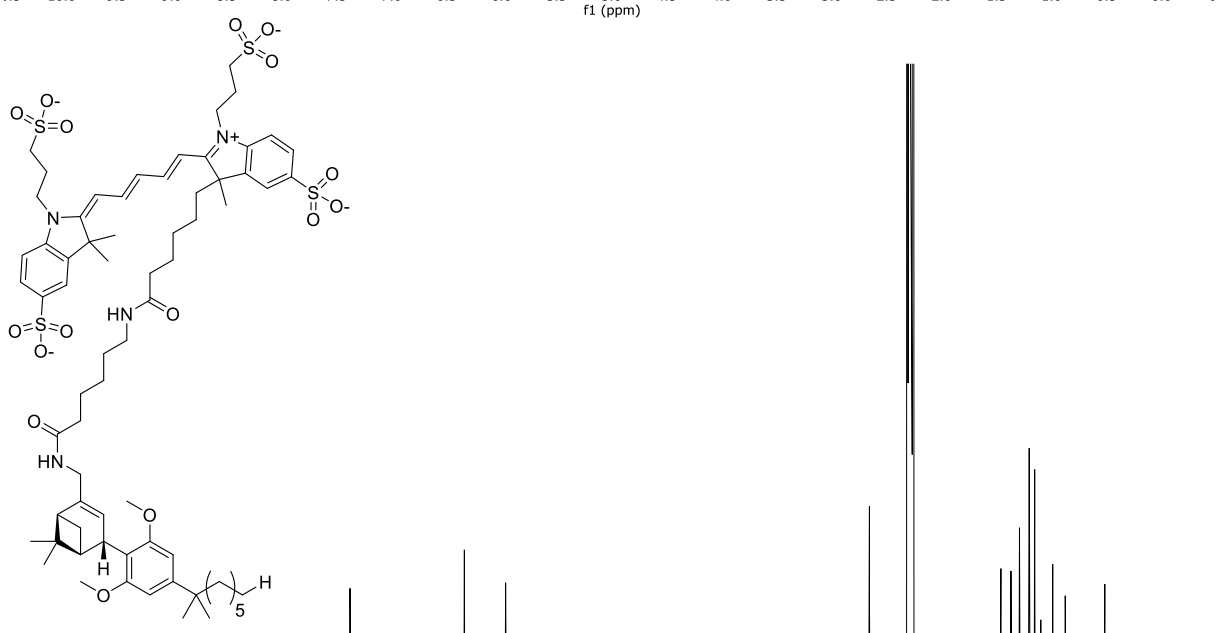

4

^{13}C NMR: 151 MHz, CD_3OD

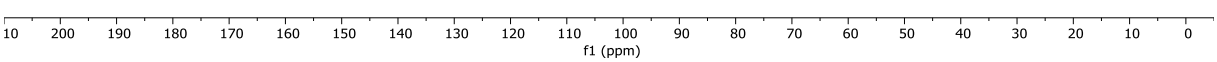

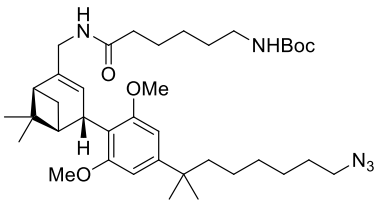

S6

^{1}H NMR: 500 MHz, $CDCl_3$

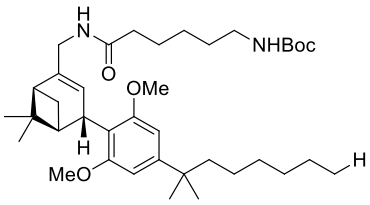

S6

^{13}C NMR: 126 MHz, $CDCl_3$

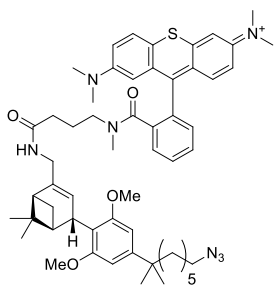

6

^{1}H NMR: 500 MHz, CD_3OD

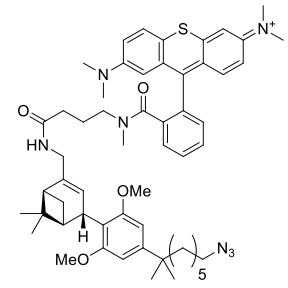

6

^{13}C NMR: 126 MHz, CD_3OD

N-TERMINAL SNAP-hCB$_2$R SEQUENCE

pcDNA4TO_SNAP-hCB$_2$R-TwinStrep-1D4 plasmid DNA sequence

GACGGATCGGGAGATCTCCCGATCCCCTATGGTGCACTCTCAGTACAATCTGCT
CTGATGCCGCATAGTTAAGCCAGTATCTGCTCCCTGCTTGTGTGTTGGAGGTCG
CTGAGTAGTGCGCGAGCAAAATTTAAGCTACAACAAGGCAAGGCTTGACCGACA
ATTGCATGAAGAATCTGCTTAGGGTTAGGCGTTTTGCGCTGCTTCGCGATGTAC
GGGCCAGATATACGCGTTGACATTGATTATTGACTAGTTATTAATAGTAATCAAT
TACGGGGTCATTAGTTCATAGCCCATATATGGAGTTCCGCGTTACATAACTTACG
GTAAATGGCCCGCCTGGCTGACCGCCCAACGACCCCCGCCCATTGACGTCAAT
AATGACGTATGTTCCCATAGTAACGCCAATAGGGACTTTCCATTGACGTCAATG
GGTGGAGTATTTACGGTAAACTGCCCACTTGGCAGTACATCAAGTGTATCATAT
GCCAAGTACGCCCCCTATTGACGTCAATGACGGTAAATGGCCCGCCTGGCATTA
TGCCCAGTACATGACCTTATGGGACTTTCCTACTTGGCAGTACATCTACGTATTA
GTCATCGCTATTACCATGGTGATGCGGTTTTGGCAGTACATCAATGGGCGTGGA
TAGCGGTTTGACTCACGGGGATTTCCAAGTCTCCACCCCATTGACGTCAATGGG
AGTTTGTTTTGGAACCAAAATCAACGGGACTTTCCAAAATGTCGTAACAACTCCG
CCCCATTGACGCAAATGGGCGGTAGGCGTGTACGGTGGGAGGTCTATATAAGC
AGAGCTCTCCCTATCAGTGATAGAGATCTCCCTATCAGTGATAGAGATCGTCGA
CGAGCTCGTTTAGTGAACCGTCAGATCGCCTGGAGACGCCATCCACGCTGTTTT
GACCTCCATAGAAGACACCGGGACCGATCCAGCCTCCGGACTCTAGGCTAGCG
CCACCATGCGGCTCTGCATCCCGCAGGTGCTGTTGGCCTTGTTCCTTTCCATGC
TGACAGGGCCGGGAGAAGGCAGCGCTAGCGATATCGGCGCGCCAGCATTTAAA
TCTGTACAGACCGGTGAATTCACCATGGACAAAGACTGCGAAATGAAGCGCACC
ACCCTGGATAGCCCTCTGGGCAAGCTGGAACTGTCTGGGTGCGAACAGGGCCT
GCACCGTATCATCTTCCTGGGCAAAGGAACATCTGCCGCCGACGCCGTGGAAG
TGCCTGCCCCAGCCGCCGTGCTGGGCGGACCAGAGCCACTGATGCAGGCCAC
CGCCTGGCTCAACGCCTACTTTCACCAGCCTGAGGCCATCGAGGAGTTCCCTG
TGCCAGCCCTGCACCACCCAGTGTTCCAGCAGGAGAGCTTTACCCGCCAGGTG
CTGTGGAAACTGCTGAAAGTGGTGAAGTTCGGAGAGGTCATCAGCTACAGCCA
CCTGGCCGCCCTGGCCGGCAATCCCGCCGCCACCGCCGCCGTGAAAACCGCC
CTGAGCGGAAATCCCGTGCCCATTCTGATCCCCTGCCACCGGGTGGTGCAGGG
CGACCTGGACGTGGGGGGCTACGAGGGCGGGCTCGCCGTGAAAGAGTGGCTG
CTGGCCCACGAGGGCCACAGACTGGGCAAGCCTGGGCTGGGTCCTGCAGGTA
CCATGGAGGAGTGCTGGGTGACTGAGATCGCCAATGGCTCCAAGGACGGTCTG
GACAGCAACCCCATGAAGGACTACATGATCCTCTCCGGCCCTCAGAAAACTGCC
GTCGCCGTGCTGTGTACTCTCCTGGGCCTGCTCTCCGCCCTGGAAAACGTGGC
CGTCCTCTACCTCATCCTGTCCAGCCATCAGCTGCGCCGCAAGCCTTCCTACCT
GTTCATTGGCTCCCTGGCCGGCGCTGACTTTCTCGCTTCCGTCGTCTTCGCCTG
CAGCTTCGTGAACTTTCACGTGTTCCACGGCGTCGATAGCAAGGCCGTCTTCCT
CCTCAAGATCGGTAGCGTGACCATGACCTTCACTGCCAGCGTGGGCTCCCTGC
TGCTGACTGCTATCGATCGCTACCTGTGTCTCCGCTACCCCCCCAGCTACAAGG
CCCTGCTGACTCGTGGTCGTGCCCTCGTCACCCTGGGCATCATGTGGGTGCTG
AGCGCCCTCGTGTCCTACCTGCCTCTCATGGGCTGGACCTGCTGCCCTCGCCC
TTGTAGCGAGCTGTTCCCCCTCATTCCTAACGACTACCTCCTGAGCTGGCTGCT
CTTCATTGCCTTCCTCTTCTCCGGCATCATCTACACCTACGGCCATGTCCTCTGG
AAGGCCCACCAACATGTCGCCAGCCTCTCCGGTCACCAAGACCGCCAAGTGCC
CGGTATGGCTCGTATGCGCCTGGACGTCCGTCTCGCCAAGACTCTGGGTCTCG
TCCTCGCTGTGCTGCTGATCTGCTGGTTCCCCGTCCTGGCTCTCATGGCTCACA
GCCTGGCCACCACCCTCTCCGATCAAGTCAAGAAGGCCTTCGCCTTCTGTAGCA

TGCTCTGCCTGATCAACAGCATGGTCAATCCCGTGATTTACGCCCTGCGCAGCG
GCGAAATCCGTTCCTCCGCCCACCATTGCCTGGCCCACTGGAAGAAGTGCGTC
CGCGGTCTGGGTTCCGAGGCCAAAGAGGAGGCTCCCCGTAGCAGCGTCACCG
AAACCGAAGCCGACGGCAAGATTACCCCTTGGCCCGATAGCCGCGATCTGGAC
CTGAGCGACTGTGGTTCCGGCCTGGAGGTCCTGTTCCAGGGTCCCGCGGCCG
CAGGATCCGCGTGGAGCCACCCACAGTTCGAGAAGGGAGGTGGAAGCGGTGG
AGGCTCAGGAGGCAGCGCATGGTCCCACCCCCAGTTTGAAAAGGGCTCAGGAG
GTAGCGAAGATCTGACCGAGACCAGCCAGGTGGCCCCCGCCTAAAAGCTTAAG
TTTAAAAAGGCTCGAGTCTAGAGGGCCCGTTTAAACCCGCTGATCAGCCTCGAC
TGTGCCTTCTAGTTGCCAGCCATCTGTTGTTTGCCCCTCCCCCGTGCCTTCCTT
GACCCTGGAAGGTGCCACTCCCACTGTCCTTTCCTAATAAAATGAGGAAATTGC
ATCGCATTGTCTGAGTAGGTGTCATTCTATTCTGGGGGGTGGGGTGGGGCAGG
ACAGCAAGGGGGAGGATTGGGAAGACAATAGCAGGCATGCTGGGGATGCGGT
GGGCTCTATGGCTTCTGAGGCGGAAAGAACCAGCTGGGGCTCTAGGGGGTATC
CCCACGCGCCCTGTAGCGGCGCATTAAGCGCGGCGGGTGTGGTGGTTACGCG
CAGCGTGACCGCTACACTTGCCAGCGCCCTAGCGCCCGCTCCTTTCGCTTTCTT
CCCTTCCTTTCTCGCCACGTTCGCCGGCTTTCCCCGTCAAGCTCTAAATCGGGG
GCTCCCTTTAGGGTTCCGATTTAGTGCTTTACGGCACCTCGACCCCAAAAAACT
TGATTAGGGTGATGGTTCACGTAGTGGGCCATCGCCCTGATAGACGGTTTTTCG
CCCTTTGACGTTGGAGTCCACGTTCTTTAATAGTGGACTCTTGTTCCAAACTGGA
ACAACACTCAACCCTATCTCGGTCTATTCTTTTGATTTATAAGGGATTTTGCCGAT
TTCGGCCTATTGGTTAAAAAATGAGCTGATTTAACAAAAATTTAACGCGAATTAAT
TCTGTGGAATGTGTGTCAGTTAGGGTGTGGAAAGTCCCCAGGCTCCCCAGCAG
GCAGAAGTATGCAAAGCATGCATCTCAATTAGTCAGCAACCAGGTGTGGAAAGT
CCCCAGGCTCCCCAGCAGGCAGAAGTATGCAAAGCATGCATCTCAATTAGTCAG
CAACCATAGTCCCGCCCCTAACTCCGCCCATCCCGCCCCTAACTCCGCCCAGTT
CCGCCCATTCTCCGCCCCATGGCTGACTAATTTTTTTTATTTATGCAGAGGCCGA
GGCCGCCTCTGCCTCTGAGCTATTCCAGAAGTAGTGAGGAGGCTTTTTTGGAG
GCCTAGGCTTTTGCAAAAAGCTCCCGGGAGCTTGTATATCCATTTTCGGATCTG
ATCAGCACGTGTTGACAATTAATCATCGGCATAGTATATCGGCATAGTATAATAC
GACAAGGTGAGGAACTAAACCATGGCCAAGTTGACCAGTGCCGTTCCGGTGCT
CACCGCGCGCGACGTCGCCGGAGCGGTCGAGTTCTGGACCGACCGGCTCGGG
TTCTCCCGGGACTTCGTGGAGGACGACTTCGCCGGTGTGGTCCGGGACGACGT
GACCCTGTTCATCAGCGCGGTCCAGGACCAGGTGGTGCCGGACAACACCCTGG
CCTGGGTGTGGGTGCGCGGCCTGGACGAGCTGTACGCCGAGTGGTCGGAGGT
CGTGTCCACGAACTTCCGGGACGCCTCCGGGCCGGCCATGACCGAGATCGGC
GAGCAGCCGTGGGGGCGGGAGTTCGCCCTGCGCGACCCGGCCGGCAACTGC
GTGCACTTCGTGGCCGAGGAGCAGGACTGACACGTGCTACGAGATTTCGATTC
CACCGCCGCCTTCTATGAAAGGTTGGGCTTCGGAATCGTTTTCCGGGACGCCG
GCTGGATGATCCTCCAGCGCGGGGATCTCATGCTGGAGTTCTTCGCCCACCCC
AACTTGTTTATTGCAGCTTATAATGGTTACAAATAAAGCAATAGCATCACAAATTT
CACAAATAAAGCATTTTTTTCACTGCATTCTAGTTGTGGTTTGTCCAAACTCATCA
ATGTATCTTATCATGTCTGTATACCGTCGACCTCTAGCTAGAGCTTGGCGTAATC
ATGGTCATAGCTGTTTCCTGTGTGAAATTGTTATCCGCTCACAATTCCACACAAC
ATACGAGCCGGAAGCATAAAGTGTAAAGCCTGGGGTGCCTAATGAGTGAGCTA
ACTCACATTAATTGCGTTGCGCTCACTGCCCGCTTTCCAGTCGGGAAACCTGTC
GTGCCAGCTGCATTAATGAATCGGCCAACGCGCGGGGAGAGGCGGTTTGCGTA
TTGGGCGCTCTTCCGCTTCCTCGCTCACTGACTCGCTGCGCTCGGTCGTTCGG
CTGCGGCGAGCGGTATCAGCTCACTCAAAGGCGGTAATACGGTTATCCACAGA
ATCAGGGGATAACGCAGGAAAGAACATGTGAGCAAAAGGCCAGCAAAAGGCCA
GGAACCGTAAAAAGGCCGCGTTGCTGGCGTTTTTCCATAGGCTCCGCCCCCCG

ACGAGCATCACAAAAATCGACGCTCAAGTCAGAGGTGGCGAAACCCGACAGGA
CTATAAAGATACCAGGCGTTTCCCCCTGGAAGCTCCCTCGTGCGCTCTCCTGTT
CCGACCCTGCCGCTTACCGGATACCTGTCCGCCTTTCTCCCTTCGGGAAGCGT
GGCGCTTTCTCATAGCTCACGCTGTAGGTATCTCAGTTCGGTGTAGGTCGTTCG
CTCCAAGCTGGGCTGTGTGCACGAACCCCCCGTTCAGCCCGACCGCTGCGCCT
TATCCGGTAACTATCGTCTTGAGTCCAACCCGGTAAGACACGACTTATCGCCAC
TGGCAGCAGCCACTGGTAACAGGATTAGCAGAGCGAGGTATGTAGGCGGTGCT
ACAGAGTTCTTGAAGTGGTGGCCTAACTACGGCTACACTAGAAGAACAGTATTT
GGTATCTGCGCTCTGCTGAAGCCAGTTACCTTCGGAAAAAGAGTTGGTAGCTCT
TGATCCGGCAAACAAACCACCGCTGGTAGCGGTTTTTTTGTTTGCAAGCAGCAG
ATTACGCGCAGAAAAAAAGGATCTCAAGAAGATCCTTTGATCTTTTCTACGGGGT
CTGACGCTCAGTGGAACGAAAACTCACGTTAAGGGATTTTGGTCATGAGATTAT
CAAAAAGGATCTTCACCTAGATCCTTTTAAATTAAAAATGAAGTTTTAAATCAATC
TAAAGTATATATGAGTAAACTTGGTCTGACAGTTACCAATGCTTAATCAGTGAGG
CACCTATCTCAGCGATCTGTCTATTTCGTTCATCCATAGTTGCCTGACTCCCCGT
CGTGTAGATAACTACGATACGGGAGGGCTTACCATCTGGCCCCAGTGCTGCAAT
GATACCGCGAGACCCACGCTCACCGGCTCCAGATTTATCAGCAATAAACCAGCC
AGCCGGAAGGGCCGAGCGCAGAAGTGGTCCTGCAACTTTATCCGCCTCCATCC
AGTCTATTAATTGTTGCCGGGAAGCTAGAGTAAGTAGTTCGCCAGTTAATAGTTT
GCGCAACGTTGTTGCCATTGCTACAGGCATCGTGGTGTCACGCTCGTCGTTTGG
TATGGCTTCATTCAGCTCCGGTTCCCAACGATCAAGGCGAGTTACATGATCCCC
CATGTTGTGCAAAAAAGCGGTTAGCTCCTTCGGTCCTCCGATCGTTGTCAGAAG
TAAGTTGGCCGCAGTGTTATCACTCATGGTTATGGCAGCACTGCATAATTCTCTT
ACTGTCATGCCATCCGTAAGATGCTTTTCTGTGACTGGTGAGTACTCAACCAAGT
CATTCTGAGAATAGTGTATGCGGCGACCGAGTTGCTCTTGCCCGGCGTCAATAC
GGGATAATACCGCGCCACATAGCAGAACTTTAAAAGTGCTCATCATTGGAAAAC
GTTCTTCGGGGCGAAAACTCTCAAGGATCTTACCGCTGTTGAGATCCAGTTCGA
TGTAACCCACTCGTGCACCCAACTGATCTTCAGCATCTTTTACTTTCACCAGCGT
TTCTGGGTGAGCAAAAACAGGAAGGCAAAATGCCGCAAAAAAGGGAATAAGGG
CGACACGGAAATGTTGAATACTCATACTCTTCCTTTTTCAATATTATTGAAGCATT
TATCAGGGTTATTGTCTCATGAGCGGATACATATTTGAATGTATTTAGAAAAATAA
ACAAATAGGGGTTCCGCGCACATTTCCCCGAAAAGTGCCACCTGACGTC

CMV promotor
serotonin 5HT3A receptor signal peptide
SNAP-tag
CB_2R
TwinStrep purification tag
1D4 purification tag

SNAP-hCB$_2$R-TwinStrep-1D4 protein sequence

MRLCIPQVLLALFLSMLTGPGEGSASDIGAPAFKSVQTGEFTMDKDCEMKRTTLDS
PLGKLELSGCEQGLHRIIFLGKGTSAADAVEVPAPAAVLGGPEPLMQATAWLNAYF
HQPEAIEEFPVPALHHPVFQQESFTRQVLWKLLKVVKFGEVISYSHLAALAGNPAAT
AAVKTALSGNPVPILIPCHRVVQGDLDVGGYEGGLAVKEWLLAHEGHRLGKPGLGP
AGTMEECWVTEIANGSKDGLDSNPMKDYMILSGPQKTAVAVLCTLLGLLSALENVA
VLYLILSSHQLRRKPSYLFIGSLAGADFLASVVFACSFVNFHVFHGVDSKAVFLLKIG
SVTMTFTASVGSLLLTAIDRYLCLRYPPSYKALLTRGRALVTLGIMWVLSALVSYLPL
MGWTCCPRPCSELFPLIPNDYLLSWLLFIAFLFSGIIYTYGHVLWKAHQHVASLSGH
QDRQVPGMARMRLDVRLAKTLGLVLAVLLICWFPVLALMAHSLATTLSDQVKKAFA
FCSMLCLINSMVNPVIYALRSGEIRSSAHHCLAHWKKCVRGLGSEAKEEAPRSSVT
ETEADGKITPWPDSRDLDLSDCGSGLEVLFQGPAAAGSAWSHPQFEKGGGSGGG
SGGSAWSHPQFEKGSGGSEDLTETSQVAPA

serotonin 5HT3A receptor signal peptide
SNAP-tag
CB$_2$R
TwinStrep purification tag
1D4 purification tag

REFERENCES

[1] D. R. Lide, CRC Handbook of Chemistry and Physics 2009-2010, 90th Edition, 2009.

[2] A. I. Vogel, Vogel's Practical Organic Chemistry 5th Edition, 1989.

[3] S. Bendels, C. Bissantz, B. Fasching, G. Gerebtzoff, W. Guba, et al., *Journal of Pharmacological and Toxicological Methods*, ASAP July 2019

[4] A. Pyka, M. Babuska, M. Zachariasz, *Acta Pol Pharm*. **2006**, *63*, 159-167.

[5] G. Jones, P. Willett, R. C. Glen, A. R. Leach, R. Taylor, *J. Mol. Biol.* **1997**, *267*, 727.

[6] Citation MOE: Molecular Operating Environment (MOE) ver. 2014.09, Chemical ComputingGroup Inc., 1010 Sherbooke Street West, Suite #910, Montreal,QC H3A 2R7 (Canada), 2015

[7] M. Soethoudt, U. Grether, J. Fingerle, T. W. Grim, F. Fezza, L. de Petrocellis, C. Ullmer, B. Rothenhäusler, C. Perret, N. van Gils, et al., *Nat. Comm.* **2017**, *8*, 1.

[8] M. Kansy, F. Senner, K. Gubernator, *J. Med. Chem.* **1998**, *41*, 1007.

[9] C. Klein Herenbrink, D. A. Sykes, P. Donthamsetti, M. Canals, T. Coudrat, J. Shonberg, P. J. Scammells, B. Capuano, P. M. Sexton, S. J. Charlton, et al., *Nat. Comm.* **2016**, *7*, 10842.

[10] H. J. Motulsky, L. C. Mahan, *Mol, Pharmacol.*, **1984**, *25*, 1.

[11] a) W. Gonsiorek, D. Heske, S. C. Chen, D. Kinsley, J. V. Jackson *et al. J. Biol. Chem.* **2006**, *38*, 28143. b) M. Bouaboula, S. Perrachon, L. Milligan, X. Canat, M. Rinaldi/Carmona, *et al. J. Biol. Chem*, **1997**, *35*, 22330.

[12] C. Yung-Chi, W. H. Prusoff, *Biochem. Pharmacol.* **1973**, *22*, 3099.

[13] A. López, N. Aparicio, M.R. Pazos *et al*. *J. Neuroinflammation* **2018***, 15*, 158.

[14] D. Wu, L. Yang, A. Goschke, R. Stumm, L. Brandenburg, Y. Liang, V. Höllt, T. Koch, *J. Neurochem*. **2007**, *104*, 1132.

[15] P. J. Murray, J. E. Allen, S. K. Biswas, E. A. Fisher, D. W. Gilroy *et al. Immunity* **2014**, *41*, 339.

[16] M. V. Westphal, R. C. Sarott, E. A. Zirwes, A. Osterwald, W. Guba, C. Ullmer, U. Grether, E. M. Carreira, *Chem. Eur. J. Chem.* **2019**, *26*, 1380.